Nanomechanical testing in drug delivery: theory, applications, and emerging trends

Sushmita Majumder¹, Changquan Calvin Sun^{2,*}, Nathan A. Mara^{1,*}

Corresponding authors

Nathan A. Mara, e-mail: mara@umn.edu

Changquan Calvin Sun, e-mail: sunx0053@umn.edu

¹ Department of Chemical Engineering and Materials Science, University of Minnesota, Minneapolis, MN 55455, USA

² Pharmaceutical Materials Science and Engineering Laboratory, Department of Pharmaceutics, University of Minnesota, Minneapolis, MN 55455, USA

Abstract

Mechanical properties play a central role in drug formulation development and manufacturing. Traditional characterization of mechanical properties of pharmaceutical solids relied mainly on large compacts, instead of individual particles. Modern nanomechanical testing instruments enable quantification of mechanical properties from the single crystal/particle level to the finished tablet. Although widely used in characterizing inorganic materials for decades, nanomechanical testing has been relatively less employed to characterize pharmaceutical materials. This review focuses on the applications of existing and emerging nanomechanical testing methods in characterizing mechanical properties of pharmaceutical solids to facilitate fast and cost-effective development of high quality drug products. Testing of pharmaceutical materials using nanomechanical techniques holds potential to develop fundamental knowledge in the structure–property relationships of molecular solids, with implications for solid form selection, milling, formulation design, and manufacturing. We also systematically discuss pitfalls and useful tips during sample preparation and testing for reliable measurements from nanomechanical testing.

Keywords

Nanoindentation; Mechanical properties; Molecular crystals; Size effect; Pharmaceutical materials; Tabletability; Amorphous solid dispersions.

1. Introduction

2324

25

26

27

28

29

30

31

32

33

34

35

36

37

38

39

40

41

42

43

44

45

46

47

48

49

50

51

52

53

The manufacturing of pharmaceutical products invariably involves solid-state processing stages, such as crystallization, transportation, storage, milling, mixing, granulation, and compression. Mechanical properties of pharmaceutical materials have a major role in the success of these processes, and yet their influence on structure-processing-property relationships is complex and still not entirely understood. Fragile crystals can fracture when drying in an agitated bed in a crystallizer, which causes poor flowability due to an excessive fraction of fines. On the other hand, when small crystals are desired for improved dissolution of drugs, size reduction by milling is more effective when the crystals are more brittle [1, 2]. More plastic materials tend to form larger bonding areas between particles during compression due to the material's ability to undergo the required permanent deformation [3]. However, excessive plasticity of drugs also contributes to a higher propensity for punch sticking during tableting [4]. More viscoelastic materials are more sensitive to an increase in tableting speed encountered during the scale up of a tablet manufacturing process due to their strain rate sensitivity [5]. Tableting behavior of mixtures depends on the mechanical properties of both drugs and excipients and their relative deformability during compression [6, 7]. To attain optimal performance during pharmaceutical processings, crystal and particle engineering have been routinely used to upgrade the properties of these pharmaceutical solids through structural modifications [8]. For crystals, improved tableting performance of bulk powders has been explained by structural features that lead to improved plasticity. In fact, the crystal structure – mechanical property relationship has been a line of active crystal engineering research since a decade ago, during which the access to accurate quantification of mechanical properties of crystals has proven essential [9]. Correspondingly, nanoindentation is witnessing an expansion in application during the past few years with its ability to test small volumes of materials with minimal sample preparation. It is an ideal technique for quantifying mechanical properties of molecular crystals, which are often too small to be routinely studied by other techniques, including tensile or compression testing. Nanoindentation allows extraction of a diverse set of mechanical properties and characterization of various mechanical properties and behaviors, including modulus of elasticity, hardness, creep rate, fracture toughness, strainhardening, phase transformations, cracking, and energy absorption [10]. Importantly, nanoindentation can also be applied mimicking operando conditions, employing heating and

cooling, controlled humidity, or even submerged specimens, providing an expanded parameter space for exploration [11]. A less well-known, but important, application of nanoindentation is the prediction of the viscoelasticity of solids. During tablet production, the deformation behavior of materials becomes highly influenced by consolidation time and press speed due to their strainrate sensitivity. Nanoindentation has been employed to generate creep data using hardness measurements, which predicts time-dependent flow of materials [12]. In addition, the continuous stiffness measurement (CSM) method in nanoindentation has proven pivotal in probing sophisticated nanomechanical properties, such as the local strain-rate sensitivity [13, 14] and creep stress exponent [15, 16]. Furthermore, hydrogels and cellulose-based nanocomposites are being increasingly used for controlled drug delivery purposes where nanoindentation can be applied to correlate the changes in mechanical properties to the amount of drug loaded [17]. Nanoindentation is highly beneficial during the pre-formulation phase of drug development where, in spite of having a finite supply of active pharmaceutical ingredients (APIs), it becomes possible to study the effect of drug composition on the mechanical performance of the manufactured tablets in a high throughput manner due to the small volumes of material involved (~1 μm³) and nearly nondestructive nature [18]. Nanoindentation is progressively used to study deformation behavior under load and correlate the crystal structure or composition to the observed mechanical performance in molecular crystals, nanopillars, microbeams, polymer nanocomposites and amorphous solid dispersions (ASDs) [19, 20].

Given the inherent scientific values and rising interest from a broadening range of researchers, nanoindentation has been the subject of a few reviews, with a focus primarily on fundamental concepts of nanoindentation and its applications in crystal engineering [21-23]. This review emphasizes the growing field of nanomechanical tests applied to pharmaceutical materials and discusses the contribution of the extracted mechanical properties in drug manufacturing. This is followed by a discussion of integration of nanoindentation with complementary techniques, such as micropillar compression, Atomic Force Microscopy (AFM) and Raman spectroscopy, to generate informationally rich datasets significantly impacting drug design and formulation.

2. Nanoindentation

85

86

87

88

89

90

91

92

93

94

9596

97

98

99

100

101

102

103

104

105

106

107

108

109

110

111

112

113

114

115

Indentation testing has a long history for quantifying hardness and quality control of materials, and has its roots in the use of the Mohs Hardness scale, where hardness was rated on a level of 1 (talc) to 10 (diamond) based upon the ability of higher ranked materials to permanently deform those of lower rank during scraping of one against the other [24]. Such an approach provided a relative measurement of resistance to permanent deformation, but lacked a foundation in measurable physical properties, such as elastic moduli, or an understanding of atomic bonding. Modern indentation testing came to existence with D. Tabor's 1951 seminal textbook entitled "The Hardness of Metals" [25], which for the first time sought to present a comprehensive physical basis for hardness measurements. Static indentation methods, such as Brinell or Vickers hardness measurements, were widely employed throughout the 20th century, and relied upon application of a known applied load and resulting size of the indent, measurable by optical microscopy. These methods yield a single indentation hardness value [26]. Although instrumented micro- and nanoindentation testing methods were developed between the 1970s-1980s, it gained popularity since 1992 when Oliver and Pharr [27] introduced an improved analytical method capable of determining mechanical properties directly from indentation load and penetration depth excluding the need for optical imaging of the indent. Over the years, further development led to the ability to measure contact stiffness allowing for continuous measurement of mechanical properties as a function of depth [28]. Moreover, improved methods were applied for calibrating indenter area functions and load frame compliances, [29] and a better understanding of the contact mechanics was established through finite element simulation [30, 31]. These developments in nanoindentation test protocols resulted in increased accuracy of data analysis and extended nanoindentation's realm of applications. During a typical nanoindentation test, the loaddisplacement profile, often called P-h curve (as shown in Fig. 1), is obtained as the material is indented with a definite loading and unloading profile using a hard indenter tip (often diamond) of known geometry.

A variety of indenter probe shapes can be used to measure elastic and plastic properties in materials during nanoindentation [32]. Since indenter shapes can significantly affect measured results, they must be considered when evaluating nanoindentation datasets. Most commonly, indenter probe types can be classified as sharp or blunt. Berkovich, cube corner and sharp conical probes are in the sharp category and vary in the angles that the faces of the indenters make with

the specimen surface normal. The face angle of a three-sided pyramid Berkovich indenter is 65.27° with a tip radius of 50-100 nm. The Berkovich probe is routinely used for hardness and modulus measurement as it is sharper than four-sided probes, is easy to calibrate, maintains a self-similar contact geometry with varying depth, and allows reliable stress measurement at very low loads [10, 32]. It is also the standard tip for nanoindenting thin films due to smaller effect of tip rounding. Another 3-sided pyramidal probe is the cube-corner, which is even sharper than a Berkovich tip, possessing a face angle of 35.3°. The cube corner tip has gained popularity for investigating fracture toughness by inducing intentional radial and median cracks in the specimen [33]. Spherical indenters are blunt tips that are widely used to accurately determine the transition from elastic to plastic contact, where very low contact depths, often on the order of a few tens of nanometers for stress-strain curve analysis are used to penetrate the specimen surface [10]. A detailed discussion of spherical nanoindentation can be found in section 4.2.1 of this review.

It should be noted that sharp pyramid indenters may pose particular challenges for probing viscoelastic behavior of materials because the strain imposed by a sharp tip can exceed the small strain assumptions of linear viscoelasticity [34, 35]. Moreover, the sharp tip produces a compliant contact for low-modulus materials that complicates precise determination of the point of contact between the indenter tip and sample surface [36]. In those cases, an axisymmetric flat punch indenter can be applied to study the viscoelastic deformation along with surface tension and creep compliance of soft materials where the contact area is not affected by the transient behavior of thermal drift [36, 37].

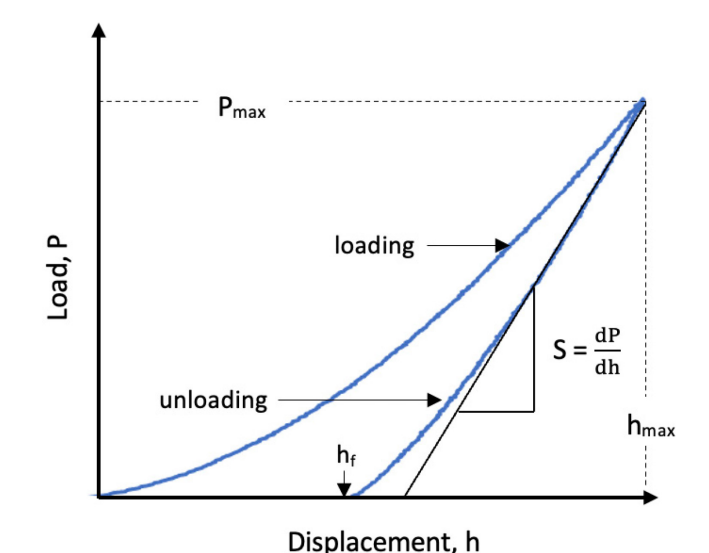


Fig. 1. Schematic representation of a P-h curve showing the loading and unloading segments, as well as the final residual displacement (h_f) and unloading stiffness S.

The most important parameters to be analyzed from a P-h curve is the unloading stiffness (S). The other quantities such as modulus and hardness (H) can be derived from the stiffness. The measured elastic modulus or reduced modulus (E_r) is given by equation (1):

$$\frac{1}{E_r} = \frac{(1-v^2)}{E} + \frac{(1-v_i^2)}{E_i} \tag{1}$$

where E and v are Young's modulus and Poisson's ratio for the material being indented and E_i and v are the same parameters for the indenter material. For most pharmaceutical materials indented with a diamond pyramidal indenter, E_i is higher than E by a factor of 1000, so the second term in the summation becomes negligibly small compared to the first. It follows that, from a practical perspective, E_r approaches E for most pharmaceutical materials of interest. Modulus and hardness can be calculated equations (2) and (3), respectively [27] where contact area (A) is the area of the residual indent impression.

$$S = \frac{dP}{dh} = \frac{2}{\sqrt{\pi}} E_r \sqrt{A}$$
 (2)

$$H = \frac{P_{max}}{A} \tag{3}$$

Furthermore, dynamic test techniques, such as continuous stiffness measurement (CSM), measures contact stiffness at any point in the loading portion of the curve rather than just from the unloading portion as in the quasi-static measurement. CSM causes a small amplitude, sinusoidal AC signal superimposed on a DC signal. The advantage of CSM lies in the fact that for a single sample experiment, continuous measurement of mechanical properties becomes possible without the need for distinct unloading cycles. Here the time constant is at least three orders of magnitude smaller compared to that of the quasi-static method, which requires determination of stiffness from the slope of an unloading portion of the curve [38, 39]. Another common dynamic test that can be performed is the strain rate jump test (SRJT), which utilizes CSM and allows a steady-state strain rate to be applied for a definite period before promptly changing the strain rate to a new value. This allows direct measurement of hardness change as a function of the strain rate in the same

indent [40], which is particularly useful for determining the strain rate sensitivity of viscoelastic materials as is relevant to high-speed tableting operations. Nanoscale Dynamic Mechanical Analysis (nanoDMA) is yet another nanoindentation approach to accurately determine the viscoelastic properties of polymers and biomaterials [41, 42]. Static indentation in the vein of Oliver and Pharr cannot be applied to quantify the viscoelastic behavior displayed by polymers because the analysis of the indentation data assumes that deformation during unloading is purely elastic in nature. In fact, any material that exhibits time-dependent characteristics will have errors in the determined modulus using static indentation. Additionally, the high compliance of soft materials means that the load on the measuring tip required to enable surface detection may have already imposed considerable deformation [43, 44]. NanoDMA involves superimposing a sinusoidal loading on the quasi-static loading during the nanoindentation test to measure the response of viscoelastic materials as a function of time, temperature, or frequency. This allow the investigation of the dynamic mechanical properties, including the storage modulus (E'), loss modulus (E''), and loss tangent (tan δ) [45].

3. Pharmaceutical applications

3.1 Molecular crystals

3.1.1 Hardness and Young's modulus

The H and E of molecular crystals measured by nanoindentation exhibit a wide range, 0.1-1.8 GPa for H and E of Pa for E [46]. The variations in E and E depend on both chemical composition of the crystal and its packing structure. Different molecular structures lead to different packing patterns in crystals and, hence, different mechanical properties. For example, the E and E values of a series of E0, E0-alkanedicarboxylic acids alternate with the number of carbon atoms [47, 48]. Both E1 and E2 of APIs can be modulated by forming multicomponent crystals, such as hydrates, salts, and cocrystals [49]. For example, hardness of the antifungal drug voriconazole could be enhanced by forming HCl and oxalate salts and softened by cocrystallizing with 4-aminobenzoic acid, 4-hydroxybenzoic acid, and fumaric acid [50]. The acesulfamate salt of an anti-diabetes drug, metformin, is significantly softer than its metformin precursor, making it more suitable for tablet formulation [51]. Even minor changes in chemical structures of cocrystal formers can similarly lead to different crystal structures and, consequently, different E1 and E2 values [52].

For a given chemical composition, different three-dimensional arrangements of molecules in polymorphs lead to different H and E [53]. In some cases, H values and aqueous solubility of different polymorphs strongly correlate, where a harder polymorph exhibits lower solubility [54]. This inverse relationship may be rationalized since a harder polymorph likely has stronger intermolecular interactions, making it energetically less favorable for release into a solution. If this relationship can be generalized, it is possible to predict relative solubility among polymorphs by nanoindentation, provided suitable single crystals can be grown. This is advantageous as some polymorphs cannot be prepared in sufficiently large quantities for solubility measurements and metastable polymorphs may transform to the more stable solid phase during the solubility experiment.

210

211

212

213

214

215

216

217

218

219

220

221

222

223

224

225

226

227

228

229

230

200

201

202

203

204

205

206

207

208

209

3.1.2 Tableting

Bonding area-bonding strength (BABS) interplay theory states that more plastic crystals provide for larger bonding areas during powder compaction, which favors manufacture of a stronger tablet [3]. Correspondingly, different solid forms of a drug exhibit different tableting performance. It was shown that the tabletability of the Form I polymorph of sulfamerazine is higher than Form II, which is consistent with the higher plasticity of Form I due to the presence of suitable slip planes in its crystal structure [55]. Similarly, polymorphs of sulfathiazole exhibit different compression properties [56]. Taking advantage of its ability to modify mechanical properties of crystals, crystal engineering has been applied to overcome pharmaceutical tabletability problems. For example, 4 salts of diphenhydramine (DPH) exhibited different H and E, as well as different mechanical behavior when bent [57]. It was shown that the more plastic acesulfame salt of DPH exhibits better tabletability, due to the larger bonding area between particles as predicted by the BABS theory. While higher plasticity generally favors better tabletability, it also correlates with higher propensity for the problem of punch sticking [4]. Thus, less deformable crystal forms (higher H) may be used when punch sticking poses a problem in tabletability [4, 58]. Given the aforementioned critical role of mechanical properties of drugs in powder compaction and tableting processes, coupled with the ability to carry out dozens of highthroughput mechanical tests on small (less than 1 mm³) and easily prepared samples, nanoindentation is becoming an important tool in guiding API crystal form selection and tablet formulation development.

3.1.3 Milling

Milling and micronization are important processes in pharmaceutical manufacturing. Sufficiently small API particles are required for ensuring drug content uniformity in tablets and capsules [59], for delivering drug to the deep lung by inhalation [60], and achieving adequate dissolution of poorly soluble drugs [61, 62]. The outcome of a milling operation depends on both the milling intensity, e.g., energy input, and mechanical properties of the material [63]. It was shown that size reduction of crystals by milling is more efficient for harder API crystals. A brittleness index, calculated from the *H* and fracture toughness obtained from nanoindentation experiments, can be used to predict the milling efficiency [1]. This was corroborated in a study of 8 pharmaceutical powders, including both APIs and common excipients, [2] supporting the possible generality of this correlation.

3.1.4 Fracture toughness

Cracks formed during nanoindentation can also be used to gain insight on the fracture toughness (K_C) of pharmaceutical solids. Though the standard method of conducting Mode I fracture toughness testing is to perform tensile testing on a pre-notched specimen, it is not always possible for organic crystals due to crystal size limitations. Nanoindentation enables characterization of both the local and bulk fracture behavior for molecular crystals [22]. Accurate, reproducible determination of K_C is dependent upon obtaining reproducible crack behavior, ideally from the corners of the indent. Crystal anisotropy can give rise to differing amounts of radial and lateral cracking vs. plastic slip as a function of indentation direction and in-plane rotation relative to the faces and corners of pyramidal indenters, making quantitative determination of K_C difficult. In some cases, such as for aspirin, in-plane rotation has a pronounced effect on hardness [64], and even spallation cracking can be observed [65]. However, if cracking geometries consistent with models can be repeatedly produced, the fracture toughness can be determined (see section 4.2.3 for examples of different cracking behaviors). Ponton and Rawlings [66, 67] developed 19 different model equations, focusing on the evaluation of fracture toughness of ceramics based on the assumption that $P/c^{3/2}$ = constant, where P is the applied load and c is the crack length. These 19 models have been tested on eight molecular organic crystals [2]: α-lactose monohydrate, acetylsalicylic acid, citric acid monohydrate, compound A, sucrose, L(+)-ascorbic acid, L(+)-

tartaric acid, and glycine, which are softer than ceramics. The study found that most of the $\ln c$ versus $\ln P$ plots of crystals yielded a slope between 0.57 and 0.78, which is close to the exponent of 2/3 for the equation $P/c^{3/2} = \text{constant}$ to be valid. However, acetylsalicylic acid, ascorbic acid and lactose showed somewhat higher slopes, which was attributed to their anisotropies. The K_C values of these molecular crystals were then determined using the Evans-Davis relationship [2]. The values of K_C for different molecular crystals of pharmaceutical interest are summarized in Table 1.

Table 1: Fracture toughness of different molecular crystals

Materials	Fracture toughness (Kc)	References
	$(MPa m^{1/2})$	
Adipic acid	0.02	[22]
Aspirin	0.004	[22]
Paracetamol	0.05	[22]
Saccharin	0.02	[22]
Sildenafil citrate	0.05	[22]
Sucrose	0.08	[22]
Voriconazole	Not measurable	[22]
α-lactose monohydrate	0.0908	[2]
Acetylsalicylic acid	0.0211	[2]
Ascorbic acid	0.0776	[2]
Sucrose	0.1083	[2]
Tartaric acid	0.1666	[2]
Glycine	0.0978	[2]

3.1.5 Mechanical anisotropy

Polymorphism is a phenomenon that is commonly encountered in the pharmaceutical industries and is rigorously monitored during manufacturing process. Different polymorphic forms potentially exhibit significantly different mechanical properties. Nanoindentation, with its site-specificity and ability to probe small volumes of material, is an ideal method for assessing location-specific mechanical response from crystal regions containing a given polymorph [68].

In addition to spatial variations in mechanical properties attributable to polymorphism, the low symmetry of molecular crystals results in directional properties and thus anisotropic behavior. Ramamurty et al. [69] studied the influence of anisotropy on mechanical response by indenting two faces, (100) and (011), of saccharin single crystals. The *P-h* curves, shown in Fig. 2, indicated a marked difference in the plastic deformation behavior as the curve for indentation on the (011) plane appeared smooth, showing homogeneous plasticity whereas indentation normal to the (100) plane showed pop-ins indicating a deformation mechanism dependent upon discrete slip.

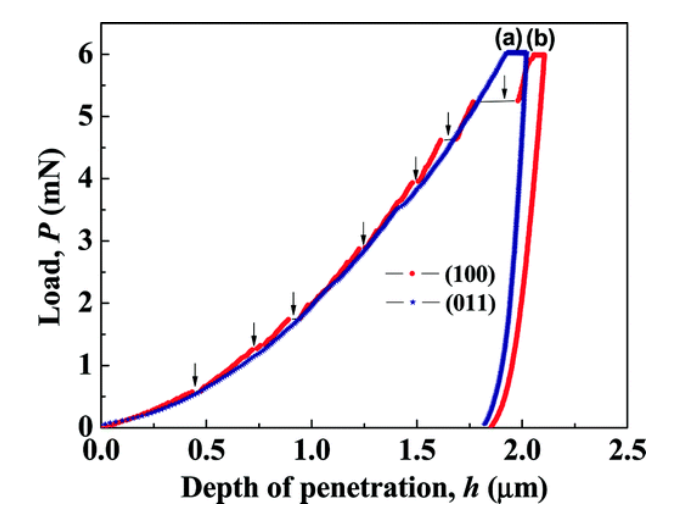


Fig. 2. Load-displacement (*P-h*) plots of saccharin with indentation perpendicular to (100) and (011) faces. Arrows show displacement bursts or pop-ins [69].

The contrasting P-h responses was attributed to the internal structure of the crystal with (011) planes consisting of numerous slip systems lying parallel to the indented plane whereas the (100) plane having the least attachment energy and acting as cleavage planes are susceptible to the displacement bursts in the P-h curve.

Ramamurty et al. [68] studied the anisotropy of two aspirin polymorphs (I and II) by nanoindentation. Among the three crystal faces examined, as seen in Fig. 3, I (100) showed the highest H (\sim 0.257 GPa) and II ($10\overline{2}$) yielded the lowest H (0.152 GPa). Here, nanomechanical testing led to the key observation that polymorph I is relatively softer than II.

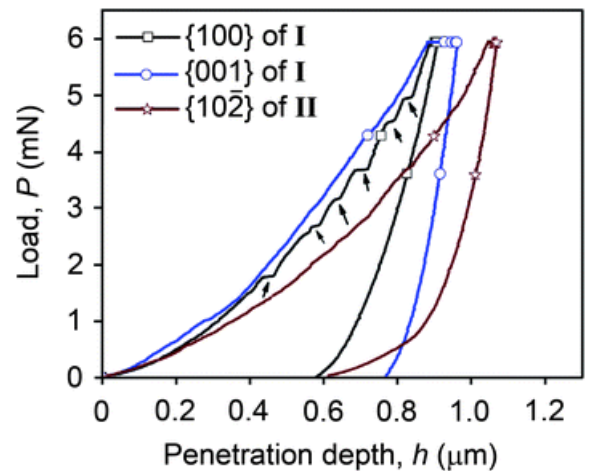


Fig. 3. *P*–*h* curves from nanoindentation on all the three faces for the aspirin polymorphs, where arrows indicate pop-ins for the loading curve of {100} in Form I [68].

Later on, the same group explained that nanoindentation has an edge over XRD in the context of resolving intergrown polymorphism due to its superior spatial resolution [70]. The group worked with three polymorphs of feldopine (I, II and III) and stated that forms I and III did not show any intergrown polymorphism but the (100) face of form II exhibited a bimodal response. Fig. 4 shows distinct clusters labelled as (100)₍₁₎ and (100)₍₂₎ obtained with 42 indents on the (100) face.

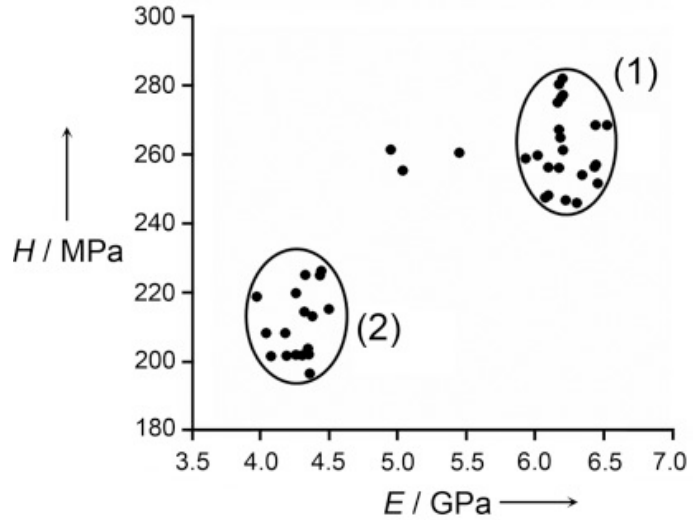


Fig. 4. *H* versus *E* obtained by nanoindentation on the (100) plane of felodipine form II, giving bimodal distribution due to intergrown polymorphism [70].

Furthermore, Ramamurty and coworkers [71] studied E and H as a function of temperature (283-343K) for saccharin and L-alanine (Fig. 5). They observed that, with increasing temperature, the E and H of saccharin and E of L-alanine were more anisotropic while the H of L-alanine was less anisotropic.

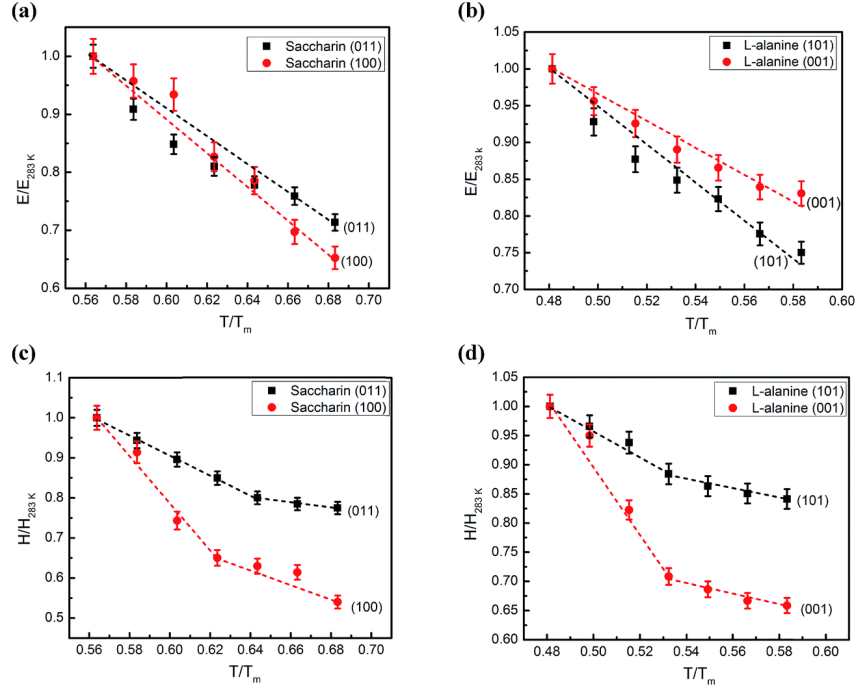


Fig. 5. Variations in both *E* and *H* on different faces of saccharin (a, c) and L-alanine (b, d) at different temperatures normalized by the respective values at 283 K [71].

3.2 Polymers and amorphous solid dispersions

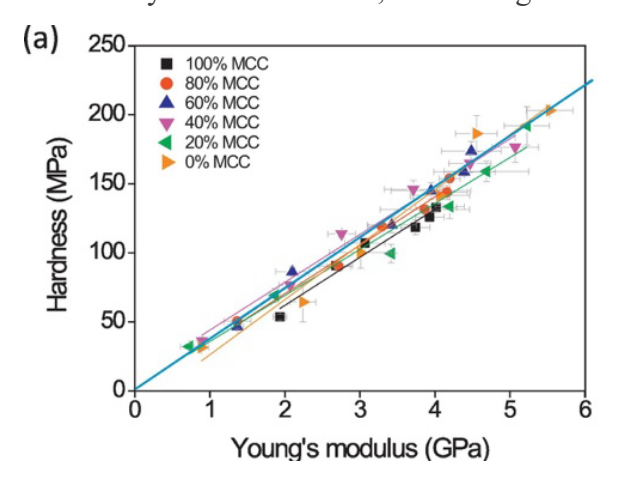
Polymer nanocomposites are multi-phase solid materials with nano fillers dispersed in the matrix. The functionality of nanocomposites is remarkably influenced by the nature of the filler and its interaction with the matrix, resulting in an unprecedented degree of change in flexibility, morphology, and interfacial characteristics, such as interfacial bonding and distribution of particles at interfaces. In pharmaceutics, there has always been a priority to incorporate the crystalline form of an API in the solid dosage due to their high degree of chemical purity and good solid-state stability. However, drugs with poor solubility exhibit low dissolution rate, which may reduce oral bioavailability [72]. A novel approach to achieving higher solubility and faster dissolution involves dispersion of the drug molecules into a hydrophilic carrier. These materials are explored intensively for both controlled drug delivery and food packaging [73]. Since mechanical response is sensitive to filler content, filler dispersion, and interfacial matrix-filler adhesion, nanomechanical testing offers sufficient spatial resolution to detect heterogeneities within the composite material as well as uneven distribution of fillers. Such information is subsequently used to improve the mechanical behavior and functionality of the drug product [74].

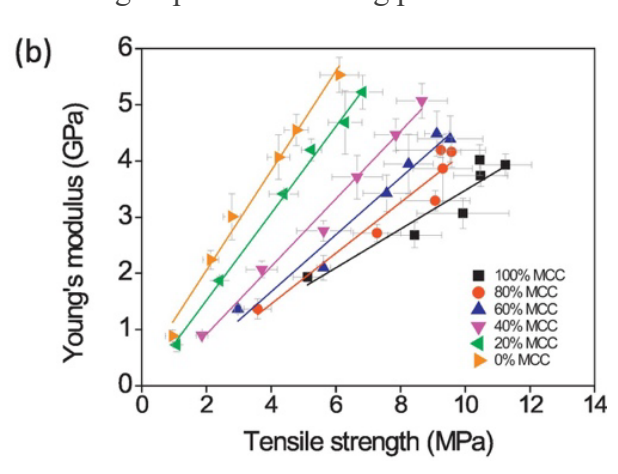
The following subsections discuss the effectiveness of nanoindentation in extracting mechanical responses from some of the most commonly used polymer-based materials in drug delivery.

3.2.1 Cellulose and derivatives

Tablets are the most desirable dosage form of drug delivery due to their combination of patient convenience and affordability. The manufacture of tablets often requires addition of excipients, such as diluents, binders, lubricants, disintegrants and glidants, in order to assist in the tablet compaction process [75] and ensure easy administration to patients. Microcrystalline cellulose (MCC) is obtained by the modification of cellulose fibers with mineral acids, and commonly used as a diluent or binder in directly compressed tablets [76].

Govedarica *et al.* [77] worked with commercial MCC, Avicel[®] PH 200 and Avicel[®] PH 101, to study the extent to which mechanical properties of discrete particles of pharmaceutical excipients control powder compressibility. Sun *et al.* [78] correlated compressibility to the modulus E, indentation H, and tensile strength (σ_t) of compacts of MCC (Avicel PH101), dibasic calcium phosphate anhydrate (DCPA), and their binary mixtures prepared under different pressures (Fig. 6). It was shown that the plastic nature of MCC led to mechanically stronger compacts at low pressures. Moreover, it was concluded that E and H were proportional to each other and independent of the material composition and, hence, one property can be predicted from the other by nanoindentation, facilitating the understanding of powder tableting performance.





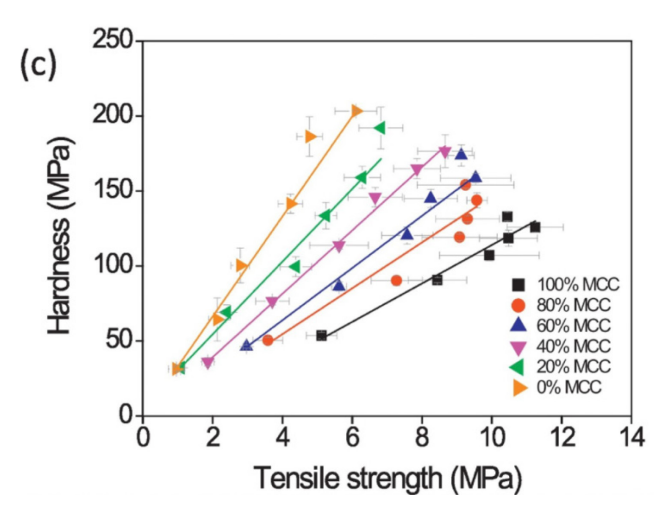


Fig. 6. Comparison and relation among hardness, Young's modulus and tensile strength of MCC, DCPA, and their mixtures (n=3). [78].

Strain rate sensitivity, or the dependence of flow stress on applied deformation rate, is an important parameter that informs tablet design through the determination of an optimal tableting processing rate. Recently, Schmalbach *et al.* [79] studied the mechanical behavior of MCC using nanoindentation and found that the strain rate sensitivity (SRS) values are in agreement with those obtained by other techniques. MCC particle sizes of 1200 µm (Vivapur® 1000) and 200 µm (Vivapur® 100) contained various degrees of porosity, with nanoindentation providing the opportunity to measure the mechanical behavior of locally dense vs. locally porous regions. Some degree of densification was observed for Vivapur® 1000 and little to none for Vivapur® 100, resulting in a depth independent modulus (Fig. 7). This indicated a homogeneous microstructure within the deformed volume. Additionally, the mean SRS of 0.046 with standard deviation of 0.004, indicated that the SRS was nearly constant across the sample. The measured modulus (3-11 GPa) and hardness yielded a broader range of values as compared to literature, [80] likely because cellulose crystallizes into several polymorphs exhibiting plastic anisotropy. Also, strain hardening effects, friction between the indenter tip and the sample, and the presence of dislocations in the plastic zone has been found to affect the measured values [81].

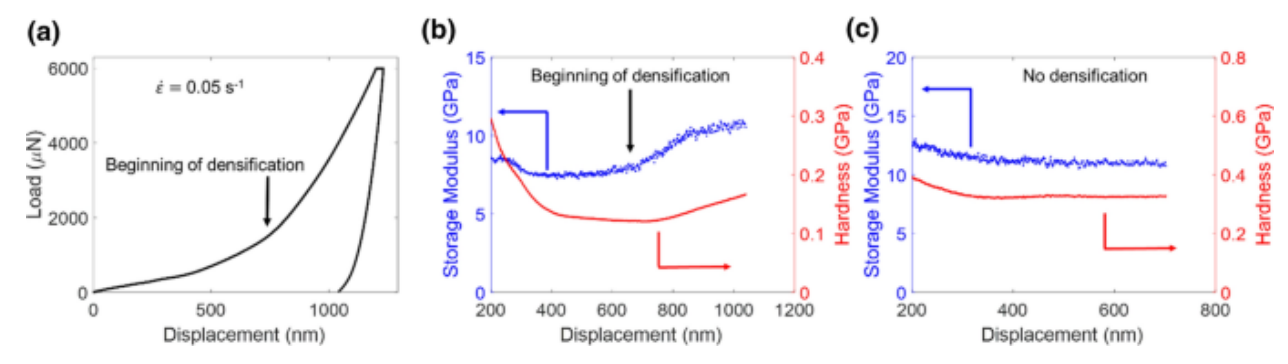


Fig. 7. (a) *P-h* curve of MCC displaying densification; (b) Depth dependence of the *H* and *E* of Vivapur[®] 1000 MCC showing signs of material densification; (c) Depth dependence of *H* and *E* of Vivapur[®] 1000 MCC not showing densification [79].

3.2.2 Starch

Starch is an extensively used excipient in the pharmaceutical industry due to its biocompatibility, biodegradability, and cost-effective traits. Being a renewable material, starch is a source of economically and ecologically sound pharmaceutical products. Apart from being used as excipients, it can also be employed as a tablet disintegrant, which triggers the release of drugs from the tablet so that they can be dissolved and absorbed. Owing to its poor flowability, modifications have been carried out, resulting in acetylated, succinylated and phosphorylated starch with enhanced pharmaceutical features [82].

Briscoe *et al.* [83] determined the mechanical properties of pre-gelatinized starch via nanoindentation after it was compressed into a tablet. The load-displacement curve (Fig. 8) showed a linear, smooth behavior with a high creep rate of about 128.46 nm/min. The smoothness of the curve and the magnitude of the creep response suggested the ductility of the material, which was ascribed to its high interior stress-strain relaxation under stress. In spite of having a high creep rate, pre-gelatinized starch exhibited poor compactibility mainly due to substantial elastic recovery during the unloading phase of compression. Thus, ductility is a necessary but not sufficient criterion for forming strong compacts.

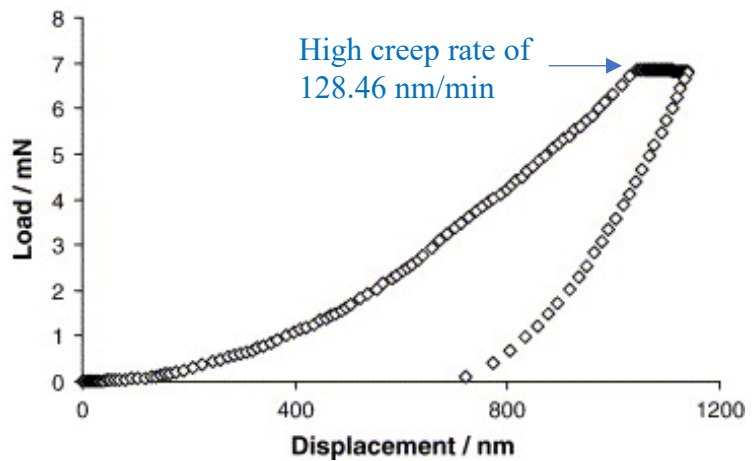


Fig. 8. A typical nanoindentation load-displacement curve for pre-gelatinized starch tablet compacted to a maximum pressure of 246 MPa [83].

Govedarica *et al.* [77] aimed to estimate the compressibility of bulk excipient powders from the mechanical properties of a single particle. The *H* (225 MPa), *E* (2.9 GPa), energy of elastic deformation (989 nJ) and energy of plastic deformation (1941 nJ) measured by nanoindentation on single particles of corn starch helped to characterize the deformation during powder compaction. For 7 pharmaceutical excipients including corn starch, a strong correlation was established between the Walker coefficient, obtained from analyzing bulk powder compression data, and single particle indentation hardness. Moreover, the energy of plastic deformation based on single particle nanoindentation studies can effectively differentiate materials exhibiting predominantly plastic deformation or brittle fracture. Thus, mechanical properties of single particles quantified by nanoindentation can be utilized to predict tablet compaction behaviors.

Starch esters have emerged as a class of potential tablet excipients for controlled drug delivery. In a recent study, Al-Zoubi [84] compared the mechanical properties of starch acetate (SA) and starch propionate (SP) to native starch (SN) by nanoindentation and correlated the material plasticity with compaction performance. The esters showed comparatively lower H (SA-87.4 and SP-41.4 and SN-238.6 MPa) and E (SA-2.1 and SP-1.5, and SN-3.9 GPa) due to a loss of crystallinity on esterification, which leads to greater plastic deformation of SA and SP than that of SN during compaction.

3.2.3 Amorphous solid dispersion

Amorphous solid dispersion (ASD) is a technique employed for improving the dissolution and bioavailability of API molecules with poor aqueous solubility. Some recent works have been performed to understand the relationship between the mechanical properties of ASDs by nanoindentation and their tableting behaviors.

Sun *et al.* [20] worked with ASDs containing acetaminophen (APAP) and copovidone to study the effect of drug loading and moisture content on the resulting mechanical behavior and tableting performance. It was observed that the hardness increased with increasing content of APAP up to 30% (w/w) and abruptly decreased at 40% (w/w). Based on nanoindentation data, it was concluded that copovidone was antiplasticized by APAP at \leq 30%. On adding a higher content of APAP, the T_g of ASD is lowered, initiating transformation from a glassy to a rubbery state at room temperature. Due to hardening of the ASD on adding APAP, it negatively impacted tablet compaction. This correlation is extremely helpful for designing robust ASD tablets.

A similar correlation was further elucidated between drug loading and its impact on mechanical properties by incorporating three drugs: ketoconazole (KTZ), griseofulvin (GSF) and peposertib (PPS) into copovidone [85]. The E increased with increasing drug contents in all cases. However, KTZ showed a comparatively weak dependence. Similarly, the increase in H by incorporation of drugs followed the order PPS > GSF > KTZ. The interplay of the impact on E and E and E and E increase in brittleness. It was concluded that, although all mechanical properties affect compressibility of the ASDs, brittle fracture plays a more dominating role. A more brittle ASD favors stronger tablets through more extensive fragmentation during compression, which leads to larger interparticulate bonding area in the compacted tablet.

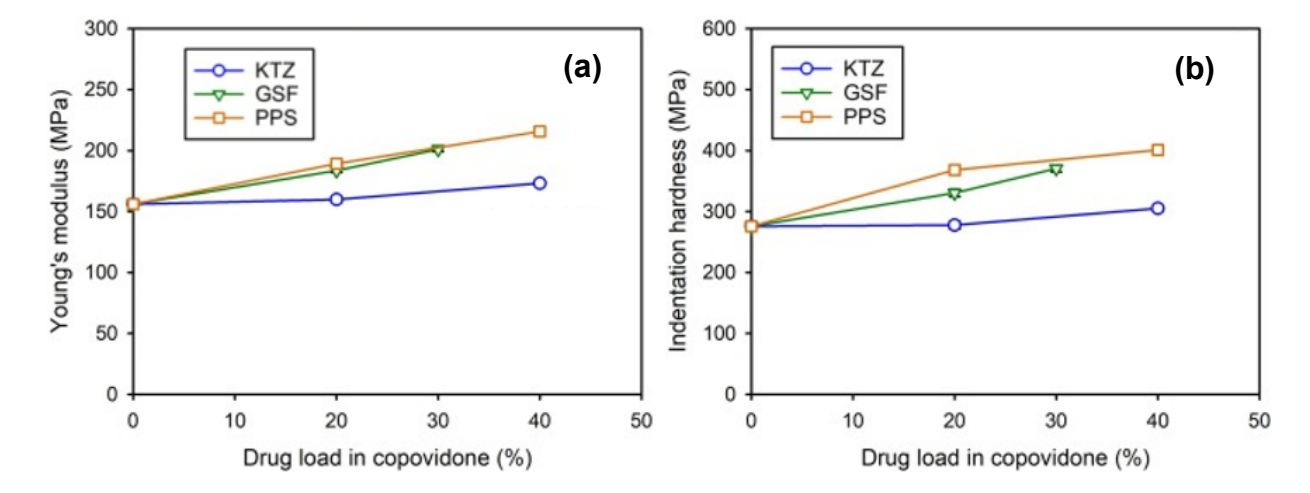


Fig. 9. a) Elastic modulus and b) hardness plots from nanoindentation as a function of loading the drugs, KTZ, GSF and PPS, in copovidone [85].

Structural relaxation is a thermodynamic phenomenon observed for amorphous materials that indicates a decrease in free energy, entropy, and free volume over time [86]. Structural relaxation has been found to impact the mechanical properties of copovidone [87], which becomes stiffer upon aging, as confirmed by higher H and E from macro-indentation experiments. However, nanoindentation revealed no significant differences between fresh and annealed copovidone (Fig. 10), indicating differing mechanical responses of the relaxed ASD at different test length scales [87].

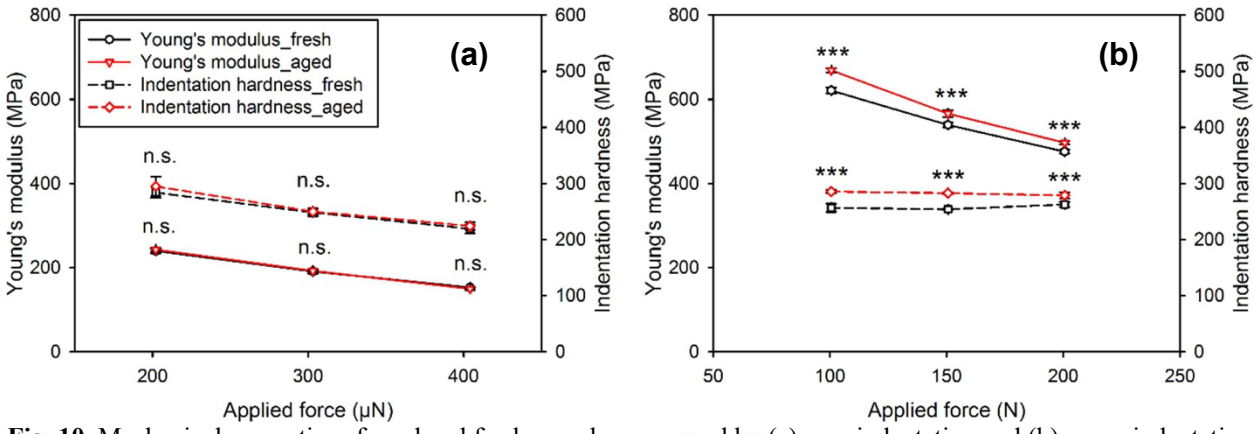


Fig. 10. Mechanical properties of aged and fresh samples measured by (a) nanoindentation and (b) macroindentation [87]. n.s. denotes that the differences between the fresh and and aged condition are either "not significant" or *** "significantly different".

3.2.4 Coating materials

Pharmaceutical film coating is a widely used step in the production of tablets to impart desired physical appearance, chemical stability, and suitable drug dissolution behaviors. Generally, polymeric coatings are applied for protective and functional performance, including preferential dissolution in the digestive tract. Since mechanical property of the coated films helps to evaluate effects of film coating on product performance, this information can also be used to optimize the film-coating process [88]. A number of analytical tools were described to assess different properties of film coatings [89] and nanoindentation stands out as a powerful method for direct mechanical analysis of the deposited film-coating, where larger scale methods are off-limits. The use of nanoindentation in extracting mechanical properties of coated films was aptly demonstrated by Perfetti et al. [90]. Sodium benzoate (Purox) was coated with two grades of hydroxypropyl methylcellulose (HPMC 603 and HPMC 615) and one grade of polyvinyl alcohol (PVA 4-98). Quasi-static and dynamic nanoindentation (nanoDMA) were performed to study the viscoelastic properties, such as storage modulus (E'), loss modulus (E'') and damping factor $(\tan \delta)$ of the coating layers. The test was carried out for two storage temperatures, room temperature and -18°C. PVA 4-98 possessed the highest resistance to quasi-static deformation followed by HPMC 603, and HPMC 615. For a storage condition of -18°C, similar trends were observed with HPMC 615 exhibiting more intense creep (2000-3000 nm) than the other coatings.

In the case of dynamic testing, as shown in Fig. 11, E' decreases in the order of PVA 4-98 > HPMC 603 > HPMC 615 and E'', which is a measure of internal damping, is higher for PVA 4-98 than that of HPMCs. The tan δ , which quantifies the ratio of viscous to elastic behavior, follows the descending order of HPMC 615 > PVA 4-98 > HPMC 603. Thus, HPMC 615 is the most viscoelastic of the three, which leads to higher ductility, flexibility and better accommodation of impact stresses. A key challenge in nanoscale dynamic testing (which is conceptually similar to bulk dynamic mechanical analysis or DMA) is the consistent knowledge of the contact area A (see equations 2 and 3), which can be affected by creep, adhesion, frictional forces, and capillarity. Because tan δ is defined by the ratio of E''/E', it represents an ideal nanoindentation measurement of viscoelasticity, since the contact area term drops out of the equation. This is reflected in the lower relative error of measured tan δ than that of the moduli (Fig. 11), indicating the greater certainty of the tan δ measurements.

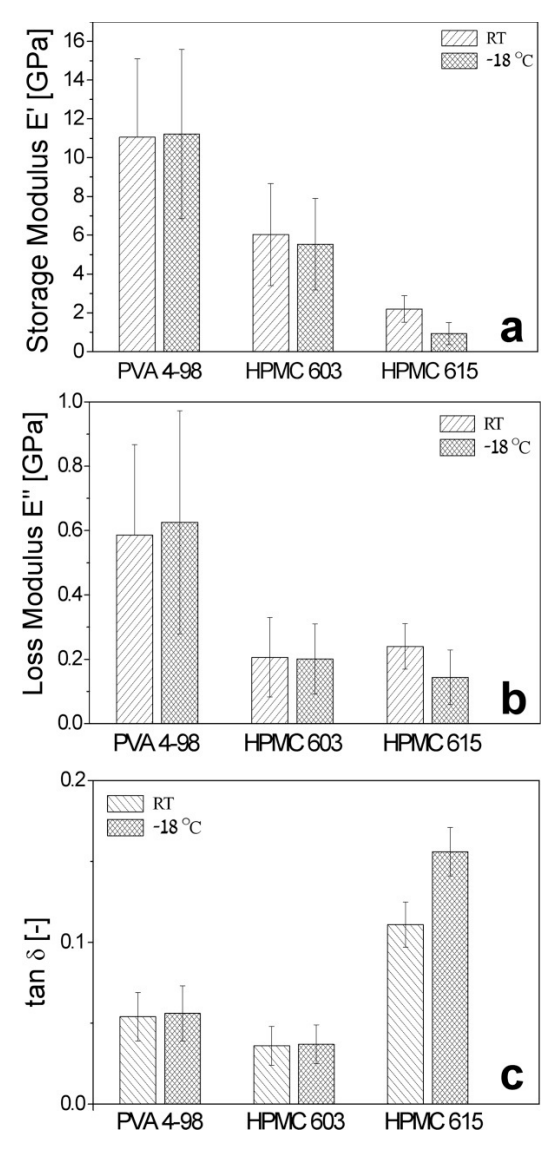


Fig. 11. Dynamic mechanical parameters (E', E'', and $\tan \delta$) obtained by nanoDMA for PVA 4–98, HPMC 603, and HPMC 615 [90].

Sun et al. [91] further corroborated the implementation of nanoindentation in selecting coating materials for drugs with poor compaction properties. They determined the yield strength and hardness of the coating material hydroxypropyl cellulose (HPC) and observed that HPC is ~41 times softer than acetaminophen (material to be coated). Thus, the coating of acetaminophen particles by the more plastic HPC significantly improved the mechanical integrity of the acetaminophen tablets by enabling a larger bonding area between adjacent particles.

3.3 Effect of temperature and relative humidity on mechanical properties

Although most pharmaceutical manufacturing processes are carried out at room temperature, Ramamurty and his group studied the temperature sensitivity of the mechanical properties in molecular crystals [92]. Their study pointed out that some thermally responsive solid-state phenomena, such as phase transformations and dislocation processes, require determination of mechanical properties with varying temperature. Nanoindentation on the major faces of saccharin, sulfathiazole form II and L-alanine at varying temperatures between 283-343K revealed that elastic modulus decreased linearly with increasing temperature which can be described by equation (4):

$$E(T) = E_0 \left[1 - \Psi(\frac{T}{T_m}) \right] \tag{4}$$

where E_0 is the intercept of the linear fit with the ordinate and Ψ is the temperature sensitivity of E, where a higher value of Ψ indicates more rapid decrease of E with T.

On the other hand, H undergoes an initial decrease with increasing temperature followed by a marked softening at an intermediate temperature range (Fig. 12). These results suggest the possibility to fine-tune manufacturing performance by manipulating mechanical properties through controlling temperatures. For instance, a material that is too difficult to process at room temperature may be tableted by raising the temperature to increase its plasticity. In fact, a mechanistic model was recently developed to address the effect of temperature on the hardness-depth relationship of single crystals by taking into account the temperature dependent lattice friction and network dislocation interaction [93].

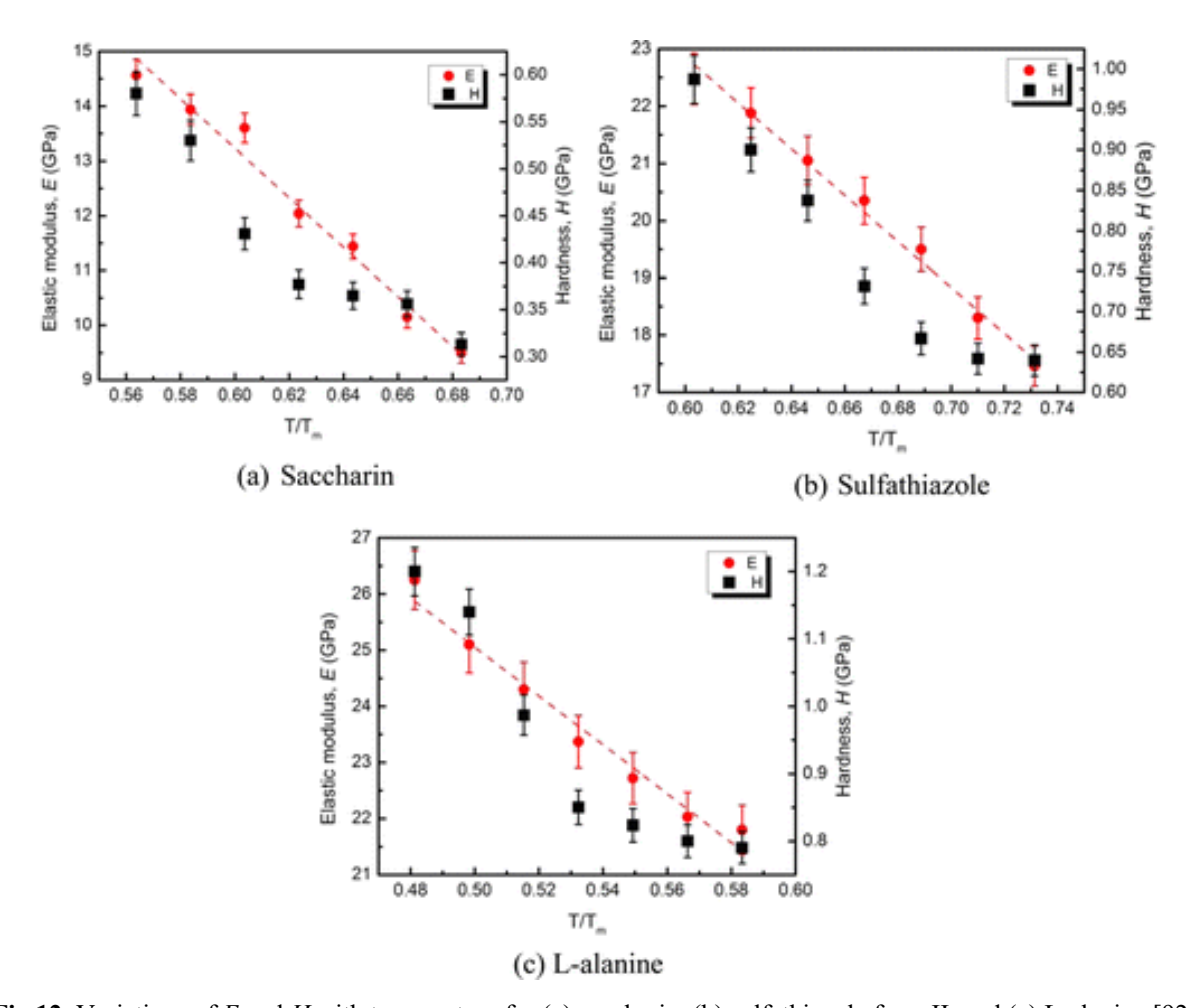


Fig.12. Variations of E and H with temperature for (a) saccharin, (b) sulfathiazole form II, and (c) L-alanine [92].

Relative humidity, RH, is another significant factor that needs to be considered during pharmaceutical manufacturing operations. RH influences the adhesion force of binders, which in turn determines the surface interactions that predict tableting performance. Nanoindentation was carried out on films composed of clotrimazole in the polymer, Kollidon VA64, at 18% and 49% RH to investigate the RH effect on the mechanical properties of ASDs [18]. Fig. 13(a) shows an increase of hardness for clotrimazole in the range of 10-60% by weight at 18% RH, whereas the hardness at 49% RH, is consistently lower than 18% RH for all compositions. Fig. 13(b) follows a similar trend with lower modulus at 49% RH along the entire composition range.

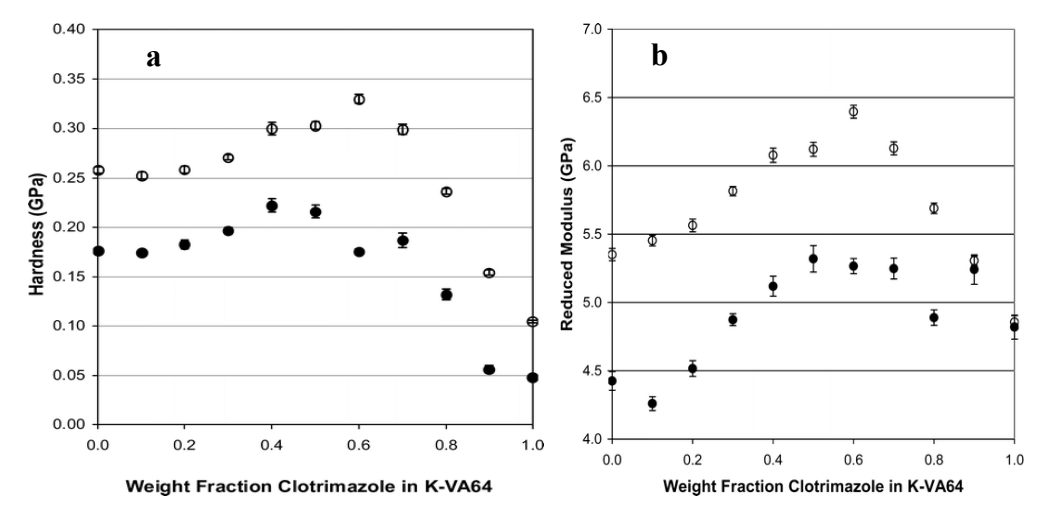


Fig. 13. (a) H and (b) E versus weight fraction of clotrimazole in K-VA64 measured by nanoindentation at 18% (\circ) and 49% (\bullet) RH [18].

The effects of RH on the mechanical properties of wood pulp fibers were carried out via AFM [94]. As evident in Fig. 14, both the hardness and modulus decrease with rising humidity, which has been linked to the swelling of the fiber.

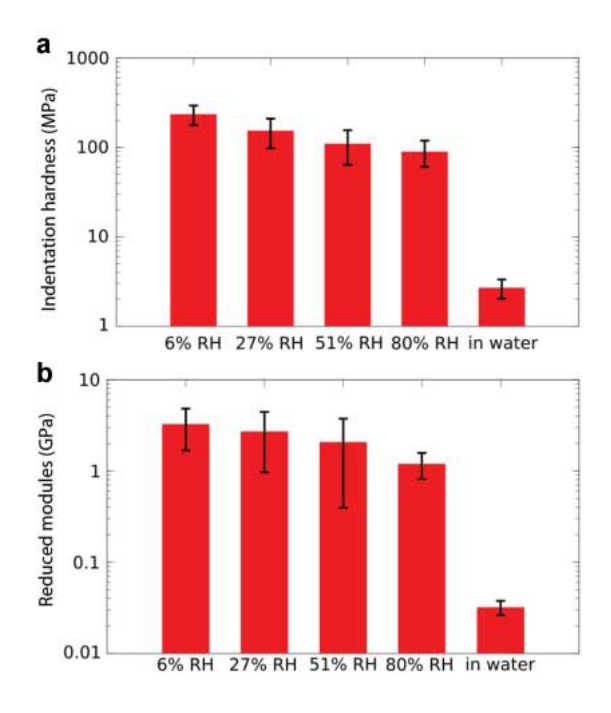


Fig. 14. (a) AFM indentation H and (b) E of pulp fiber surfaces at varying RHs and in water [94].

In another study by Sun and coworkers [20], it was observed that, as the content of acetaminophen (APAP) is increased in copovidone, the *H* is initially increased for small fractions of APAP, then reduces when APAP content further increases. Furthermore, an increase in humidity was always accompanied by a lower *H* for the same amount of APAP (Fig. 15).

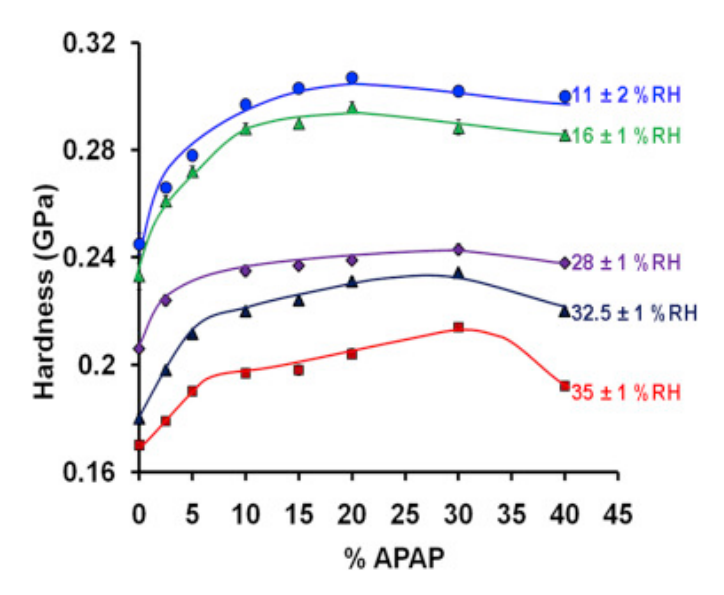


Fig. 15. Hardness of APAP-copovidone ASD as a function of APAP content and RH [20].

4. Challenges and recent developments in nanomechanical testing

4.1. Challenges resulting in errors during nanoindentation

So far, it is clear that nanomechanical testing has proven to be a robust tool for determination of key mechanical properties in pharmaceutical products. Nanoindentation in particular is conceptually simple, i.e., 1) press a hard tip of known geometry into a surface, 2) measure load and displacement, and 3) analyze the load-displacement curve. The first two concepts require only a smooth, flat sample surface, and equipment with the necessary load (down to a few piconewtons) and displacement (sub-nanometer) resolution. In contrast with uniaxial testing, which requires comparatively complex sample geometries and extensive machining and grip configurations, nanoindentation offers the benefits of convenient data collection at the expense of increased complexity in data analysis to account for the complex stress state beneath the indenter and to calculate the relevant material properties in a way that can be compared to values obtained via uniaxial loading.

There are three main sources of error that must be corrected for when analyzing data for a typical nanoindentation test. Fig. 16 shows the quantities that should be corrected: (a) estimation of the point of contact between the indenter tip and sample (zero point), (b) the load frame compliance, and (c) the indenter contact area function [95].



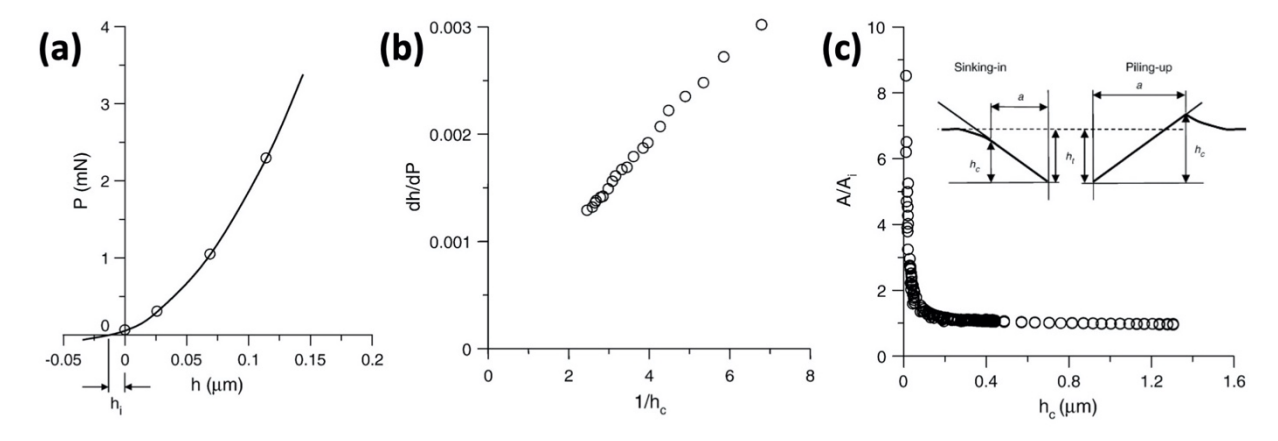


Fig. 16. (a) Typical initial portion of a P-h curve in nanoindentation where an offset h_i in initial contact between tip and indenter must be accounted for. (b) Plot of the sample and load frame compliance vs. the inverse of contact depth. Here, the y-intercept will give the value of the frame stiffness. (c) Plot of the contact area, A, normalized by an ideal contact area for a perfect Berkovich pyramidal tip as a function of contact depth. Note the significant deviation from ideality at low contact depths arising from tip rounding. Inset shows deviations from assumed contact area due to pile-up or sinking-in of material around the indenter [95].

Identifying the initial point of contact is a particular challenge when testing pharmaceutical materials. Oftentimes, the automated analysis software will choose a zero point that upon examination deviates a few nanometers (h_i in Fig. 16(a)) off of the true point of contact. One possible reason for the error in identifying the initial point of contact is tip contamination. A contaminated tip, due to material adhering on the tip from a previous indentation test, leads to premature data collection once the tip contaminant is in contact with the sample surface. These can easily lead to substantial error in calculation, as the calibrated contact area, A, is an exponential function of contact depth, where small deviations in h can cause large errors at greater depths. To minimize this error, cleanliness of the indenter tip should be periodically checked by indenting a standard material, e.g., fused silica. If the measured value is different than that expected, the tip should be cleaned via placing deep indents in a soft material, such as polycarbonate or styrofoam. Other reasons can be problems with accurately determining the contact setpoint load, including moving from one indent to another on a highly tilted sample, or poor calibration of the load transducer.

Accurate determination of the equipment frame compliance (Fig. 16(b)) also can be an issue. The frame compliance is generally calculated using a very solidly mounted reference standard, such as fused silica, under relatively high loads where all compliance outside of the material indentation itself is assumed to be equipment-related and is fit by plotting against $1/h_c$ as in Fig. 16(b). This assumption holds during subsequent testing if the pharmaceutical sample is equally well-mounted. If so, the effect of errors due to machine compliance is small since the modulus of most pharmaceutical materials is relatively low. Unfortunately, the small size of some pharmaceutical crystals makes secure mounting a particular challenge. If there is any compliance from mounting adhesives (thick glue lines are a frequent source of compliance), or other sources not present during the compliance calibration, significant errors in hardness and modulus can arise, leading to unreasonable high E and H values.

Contact area errors are also a major source of discrepancy in nanoindentation data. Fig. 16c shows a plot of the measured contact area for a Berkovich pyramidal indenter normalized by the area of a perfect indenter A_i plotted with varying contact depth. At shallow indenter depths the deviation between measured and ideal contact area becomes large. This arises from the fact that real indenter tips are not infinitely sharp, but rounded with a ~50-100 nm radius at the tip. As such, measurements at low depths require additional calibration to account for the transition from a pyramidal geometry to one that is more rounded. Pharmaceutical crystals can be prone to cracking at large indentation depths, which often limits experiments to low contact depths. For small indentation depths, an increased number of calibration data points should be taken over the relevant depth range, which may require multiple calibration indents spread over a broad depth range to obtain a full area function calibration over the chosen load range of the indenter equipment.

Pharmaceutical materials pose other unique challenges to nanoindentation measurements. Fracture is a concern for brittle materials, where radial cracking can lead to lower measured stiffnesses. This in turn will affect modulus and hardness values, as the indentation depths will be greater for a given load than for a non-fractured sample. Atomic Force Microscopy (AFM) utilized post-indentation can image such cracks, and subsequent tests can be carried out below the critical load for fracture. Modern nanoindentation equipment often offers the option to use the indentation probe in a similar way as an AFM to collect topographic maps of indents via scanning probe microscopy (SPM), which alleviates the need to use separate AFM equipment to detect cracking. The inset of Fig. 16c shows another issue that affects assumptions regarding contact area. During

fully elastic deformation, a certain amount of sink-in is expected, but generally results in lower error than that for material pileup as seen in deformable materials, such as many of those commonly found in the pharmaceutical industry. As material is plastically deformed, it may result in pileup of material around the indenter. The pileup supports some of the indentation load, thereby giving an artificially low h_c for a prescribed load P, which results in both a higher measured modulus and hardness. The most direct way to correct for this effect is to conduct AFM scans of the indent and measure the contact area directly. Somewhat less time consuming is conducting a tip area function on a known standard that undergoes pileup in a similar fashion as the sample of interest.

4.2. Emerging trends and test methods

4.2.1 Spherical nanoindentation stress-strain curves

Indentation-based methods can provide more information than simply modulus and hardness. Spherical indentation stress-strain protocols have been refined over the past two decades to provide the full indentation stress-strain curve under indentation conditions. Such methods have been used extensively in metals, and date back to Tabor's original text [25], where a spherical indent with a given load was made into a material, and the contact area subsequently measured directly via optical microscopy. This was repeated for many indents at different loads, with each representing a data point on a stress-strain curve. New advancements and the introduction of fully instrumented, automated nanoindentation equipment (for a review, see [96]) have facilitated development of advanced protocols for the zero point correction, a new definition of indentation strain, and demonstration of effectiveness to test a wide range of materials, including ion irradiated metals [97], highly anisotropic metals [98], mouse bone [99], and carbon nanotube brushes [98].

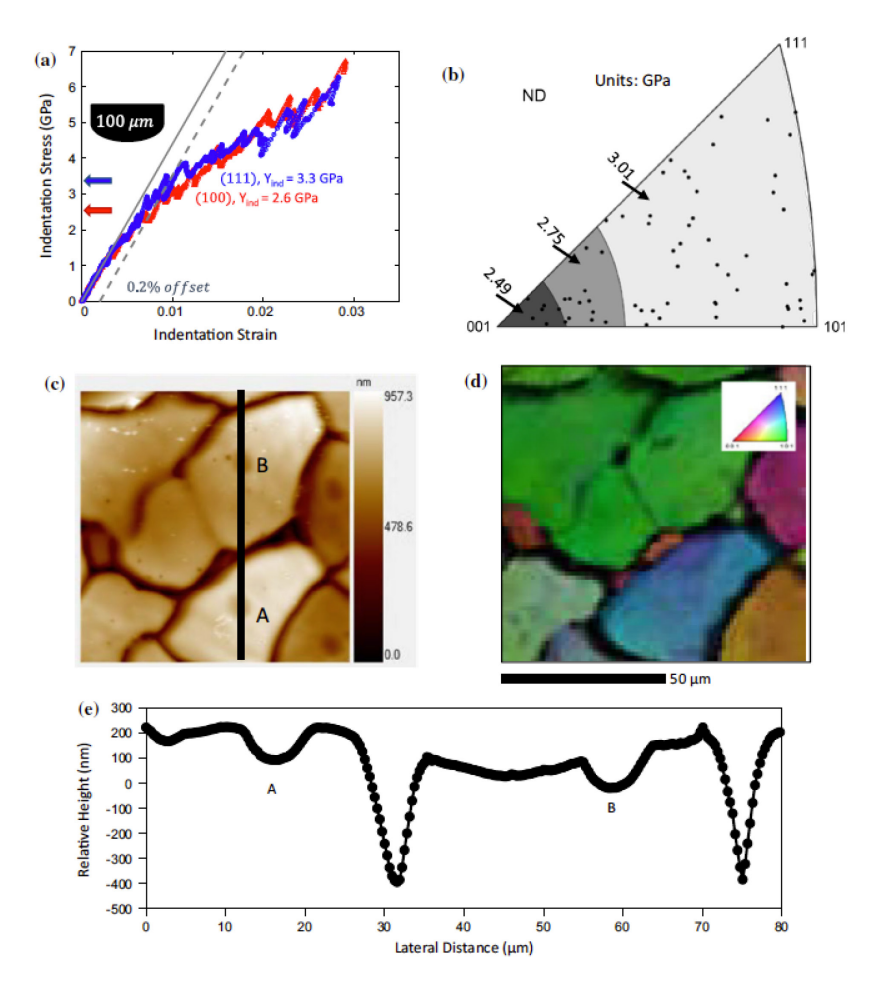


Fig. 17. (a) Indentation stress–strain curves for 100-□m indenter on annealed tungsten for grains with indentation directions near [100] and [111] crystal directions. (b) An inverse pole figure (IPF) contour map. Each black point is a grain with 1–2 tests. (c–d) Depth contour map from low force scanning with Berkovich tip and corresponding IPF-IQ (image quality) map. (e) Depth profile along highlighted line across indents [97].

Using the protocols detailed in [96], indentation via a 100-mm radius diamond spherical tip was conducted on Tungsten (W). Fig. 17(a) shows the indentation stress-strain curves for two differently oriented grains. Here, the elastic anisotropy is minimal, as expected for W, and indenting normal to the (100) and (111) grains give the proper trend in yield strength with changing orientation for body centered cubic materials (Fig. 17b). The SPM scan in Fig. 17(c) and corresponding Electron Backscatter Diffraction (EBSD) map in Fig. 17(d) provides both topographic data (see Fig. 17(e) for a line profile) and crystallographic orientation. These indentation stress-strain protocols may also be applied to pharmaceutical crystals to provide detailed site-specific indentation data beyond the hardness and modulus data generally determined via pyramidal (Berkovich) indentation. However, it must be kept in mind that under spherical indentation conditions, the elastic region and yield point occur within the first few tens of

nanometers depth after contact, so minimizing surface roughness effects can pose a challenge. Potential applications include investigation of crystal anisotropy effects, polymorphism, deformation near bicrystal boundaries, and determination of the elasto-plastic transition to a higher degree than that afforded by pyramidal indentation.

674

670

671

672

673

675

676

677

678

679

680

681

682

683

684

685

686

687

688

689

690

691

692

693

694

695

696

697

4.2.2 Uniaxial testing

Another major challenge with indentation-based measurements is understanding the complex triaxial stress state under an indenter, which may include shear, compression, and tensile components, that change as a function of position under the indenter. Uniaxial deformation, with all its difficulties in sample preparation and test execution is much easier to analyze. Over the past two decades, uniaxial micropillar compression has been extensively used in metals, intermetallics, ceramics, and their composites to determine the full stress-strain response. Micropillar compression requires the use of Focused Ion Beam (FIB) milling to machine a pillar of known dimension (Fig. 18(a)). The volumes of material involved are roughly equivalent to those found for nanoindentation, though with a uniaxial stress state, calculating the stress-strain curve as in Fig. 18(b) is more straightforward than for spherical nanoindentation, and the onset of shear instabilities or cracking can be readily observed if the experiment is carried out in-situ in the Scanning Electron Microscope (SEM). As for spherical nanoindentation, expanding these techniques into pharmaceutical materials has challenges associated with sample preparation. FIB utilizes an ion beam (here, gallium ions Ga⁺) to bombard the surface and sputter away those atoms or molecules to be removed in the subtractive machining process. FIB machining leaves behind a certain amount of ion beam damage on the sample surface, consisting mainly of amorphous material and implanted Ga that may penetrate 10s of nm into the sample. For smaller pillars where the surface area to volume ratio is high, the fraction of damaged material becomes progressively higher. For pharmaceutical materials, the degree of FIB damage has not been widely quantified, nor has its effects on the resulting mechanical properties. Nevertheless, microscale techniques that also include bend testing, pillar splitting [100], and tension [101] may be applied to future pharmaceutical material studies to obtain the full stress-strain response of small volumes under a relatively straightforward stress state, or to determine fracture toughness.

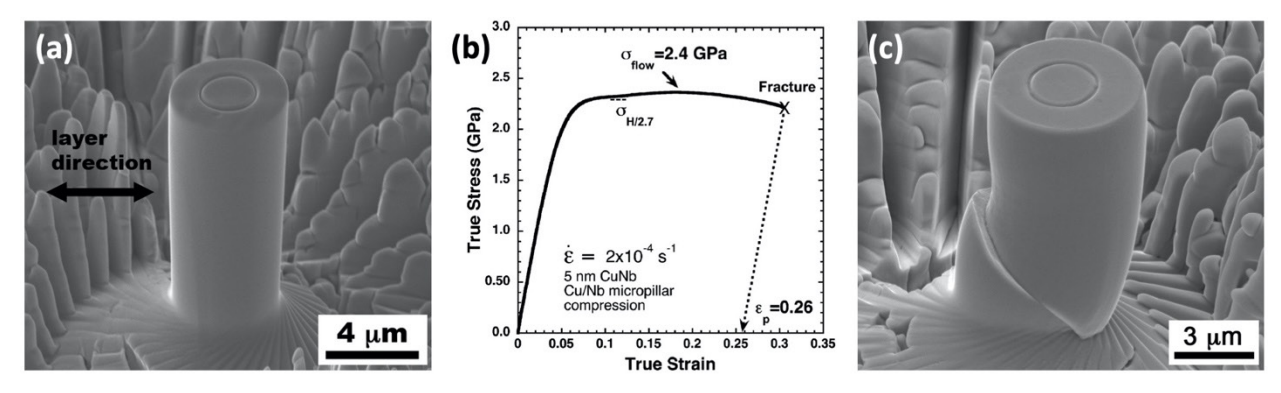


Fig. 18. (a) Micropillar of a nanolamellar Cu-Nb composite manufactured via Focused Ion Beam (FIB) milling. (b) Compression stress-strain curve for Cu-Nb nanolamellar material of 5 nm layer thickness. Note that the Hardness divided by a Tabor factor of 2.7 from nanoindentation experiments closely correlates with the measured flow stress. (c) Micropillar in (a) after deformation to 0.25 plastic strain. A shear instability has formed at the end of the test, as shown by the stress-strain curve in (b) [102].

4.2.3 Determination of rate dependency of fundamental unit deformation mechanisms

The multiple pop-in events observed when nanoindenting molecular crystals correspond to intermittent plasticity or crack propagation in these crystals. Strain-rate sensitivity (SRS) has no role in the appearance of these pop-ins for these molecular crystals as shown by Ramamurty et al. [103]. They observed that the calculated strain rate sensitivity for molecular crystals is close to zero and the measured H is independent of SRS exponent (m) (see Fig. 19 below). This is because the intermolecular interactions in these crystals are considerably weaker than those found in metals and can be broken easily. As a result, plastic deformation in molecular materials does not require dislocation motion, rather slip occurs through shearing of specific crystallographic planes. This deformation is also favored by the larger free volume and lower packing efficiencies in molecular crystals as compared to those found in metals. Using detailed analysis of discrete displacement bursts, they found that the pop-in lengths observed during the loading segment of nanoindentation correspond to an integer multiple of inter-planar spacing of the slip planes, consistent with shear sliding of the crystallographic planes as being responsible for the multiple pop-ins and plasticity in molecular crystals [69, 104]. Little work has been done to relate the strain-rate sensitivity to fracture initiation.

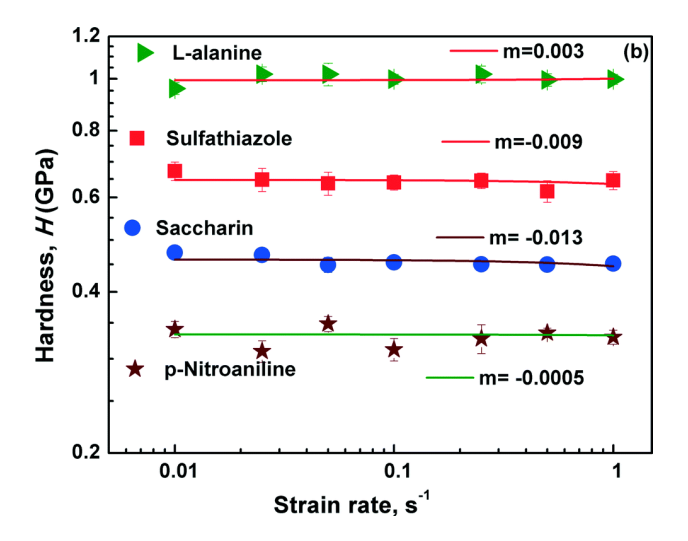


Fig.19. Strain rate insensitivity of the measured hardnesses for different crystals [103].

Nanoindentation has now gone beyond measuring the conventional modulus and hardness of a material and is capable of probing thermally activated deformation process, which provides information on strain-rate sensitivity (SRS) and activation volume [105]. Nanoindentation has become a frequent tool to determine SRS, especially for ultrafine-grained and nanocrystalline materials. Several tests and approaches have been discussed in literature for nanoindentation SRS measurements. An advanced nanoindentation protocol, strain rate jump test (SRJT) was developed [14] where a standard CSM method was modified to perform abrupt strain-rate changes at defined indentation depths during one single indentation. Mayo and Nix [106] determined a SRS exponent (*m*) with constant loading rate and deduced the following expression:

738
$$m = \frac{\partial \ln \sigma}{\partial \ln \dot{\epsilon}} \sim \frac{\partial \ln H}{\partial \ln \dot{\epsilon}} = \frac{\partial \ln H_2 - \partial \ln H_1}{\partial \ln \dot{\epsilon}_2 - \partial \ln \dot{\epsilon}_1}$$
 (5)

Here, σ is the plastic stress and \dot{E} is the applied strain-rate. Additionally, SRS can also be expressed in terms of activation volume (V), Boltzmann constant (k), absolute temperature (T) and H as:

$$m = \frac{3\sqrt{3} kT}{V \cdot H} \tag{6}$$

Activation volume is defined by Gibbs [107] as the volume being involved during the unit deformation. In molecular crystals, plastic deformation can be considered a transition from one state to another through an intermediate activated state under the application of stress. As a result, activation volume is the product of the activation area (product of the dislocation length and the

Burgers vector, b) and the distance to overcome due to an obstacle and expressed in units of b^3 . Since molecular crystals are strain-rate insensitive, as discussed above, V cannot be determined using equation (6) due to the presence of strain-rate sensitivity exponent (m) there [108]. Hence an alternate way of estimating V is to observe the statistical distribution of stress required for incipient plasticity. This can be accomplished by performing nanoindentation using a spherical indenter. A model developed by Schuh and coworkers [109, 110] can be applied to examine the statistical nature of the first pop-in loads which in turn can determine the V from the following equation:

756
$$V = \frac{\pi}{0.47} \left(\frac{3\rho}{4E_R}\right)^{2/3} \text{ kT. } \alpha \tag{7}$$

758 Where ρ is the indenter tip radius, α is the fitting parameter and ER is the reduced modulus.
759 Recently, activation volume determination was carried out for microcrystalline cellulose (MCC)
760 [79], a frequently used excipient for drugs and dietary supplements, using the equation

$$V = C \sqrt{3kT} \frac{\partial \ln \dot{\varepsilon}}{\partial H}$$
 (8)

Where C is the Tabor factor, a constant, considered to be 2 for MCC.

In this work, SRS was determined via indentation SRJT and the average SRS for quasistatic strain rates was found to be 0.046, with an activation volume equal to 1.05 nm³. In metals, the activation volume corresponds to the average volume swept by a dislocation in overcoming an obstacle [109, 110]. A physical representation of activation volume in molecular crystals is much more elusive, and the quantitative impact of this value is difficult to interpret.

4.2.4 Detecting indentation-induced fracture without post-indent imaging

Nanoindentation-based methods for investigating fracture phenomena have their roots in understanding the shaping of brittle materials by fragmentation or milling, and efforts to understand the effects of concentrated loads on fracture have been intensively studied for decades. For a complete review of the classic fracture mechanics approaches, see the seminal work by Lawn and Wilshaw [111]. These approaches are best applied to large indents in transparent solids, where optical observation of the subsurface crack geometry leads to reliable application of the proper fracture model. For pharmaceutical materials investigated via nanoindentation, observation of the

crack geometry is often elusive due to the opaque nature of the material or the small size of the cracks, although researchers often still utilize nanoindentation to examine the propensity to fracture [112]. Despite the influence of crystal anisotropy and crystalline defect content, a value for K_c may be calculated by subsequent measurement of crack length originating from the residual indent, and knowledge of the material H and E [1]. This can then be used for a calculation of the brittleness index, defined as the ratio between the hardness and K_c as calculated per the Lawn and Marshall approach [113] enabling qualitative ranking of the relative millability of pharmaceutical materials [1]. This is an extremely useful, if not mechanistically descriptive, tool for pharmaceutical material design. Nevertheless, it is well known that if cracking occurs, the assumption of Hertzian contact that underpins the Oliver-Pharr method for hardness and modulus no longer holds, and the unloading curve after cracking will differ from that of a sample that did not undergo cracking. This difference in unloading stiffness has been exploited by Morris et al. [114] to detect the occurrence of cracking without the need for optical characterization, opening the potential for higher-throughput crack detection. Here only a comparison in the unloading slopes for two different geometry pyramidal indenters (e.g. Berkovich vs. cube corner) is needed. They found that their unloading-curve analysis approach could even detect cracks when no pop-in events were evident in the loading curve. Burch et al. utilized this unique approach for idoxuridine as seen in Fig. 20 [115].

779

780

781

782

783

784

785

786

787

788

789

790

791

792

793

794

795

796

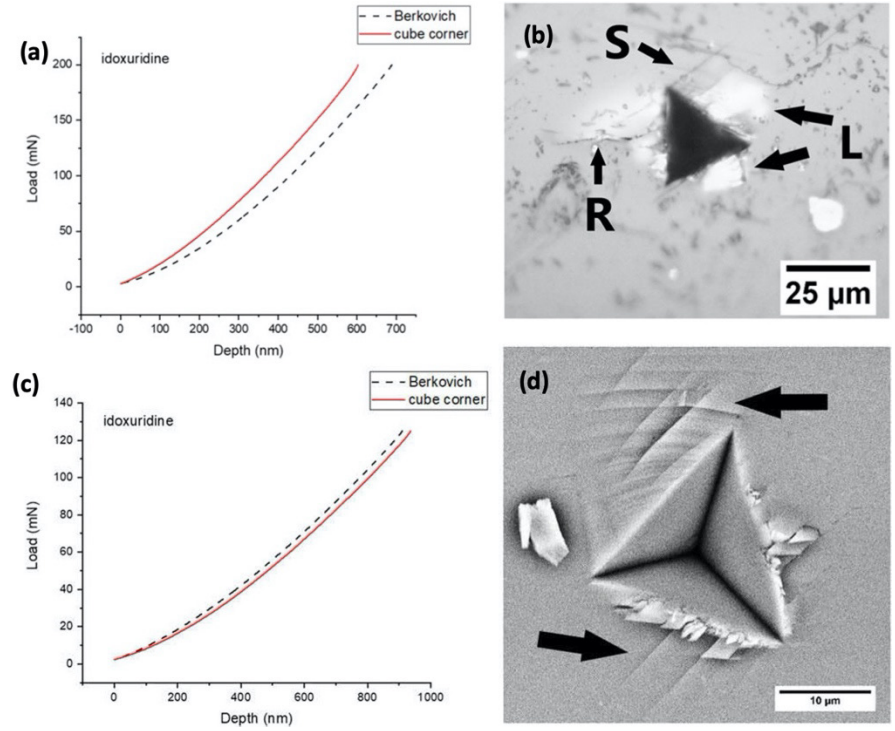


Fig. 20. Detecting the presence of radial cracking during nanoindentation of idoxuridine. (a) Offset unloading curves for Berkovich and cube corner indents in the presence of radial cracking. Note that the two curves do not superimpose. (b) Corresponding cube-corner indent where radial cracks are denoted by R, lateral fractures L, and slip lines S. (c) Offset unloading curves for Berkovich and cube corner indents that superimpose. (d) Corresponding cube corner indent where slip bands are present, denoted by arrows, but no cracking occurs [115].

The unloading curve analysis protocols proved to be a reliable method of detection of radial cracks, where the predictions held up to visual inspection for 94% of results, with all deviations being false negatives, where the curves superimposed, but cracking was visually evident. The authors went on to calculate toughness values using existing models by Jang and Pharr [116] and Morris and Cook [117]. However, due to the complex crack geometries where fracture may not initiate from indent corners, and the effects of small variations in the in-plane crystal rotation relative to the indenter tip coupled with crystal anisotropy, the authors concluded that the application of the fracture models to be appropriate for first order estimates of toughness.

4.2.5 AFM based investigation of nanomechanical behavior

In general, AFM based techniques are carried out at lower loads, and with sharper tips than those found in nanoindentation, although tip/cantilever combinations are available for AFM that can approach the sizes and loads found in nanoindentation of softer materials. AFM based techniques are particularly useful for determining near-surface properties of materials that necessitate smaller indentation depths than nanoindentation provides. However, smaller indent

depths and lower loads bring other issues that must be overcome, such as an increased relative effect of sample roughness, and limitation of indenter sizes and shapes suitable for testing to sharper tips, such as cube-corner geometries. In a comparative study between material types, Masterson and Cao evaluated the particle hardness of four pharmaceutical materials via AFM indentation techniques. They found that for sucrose, lactose, ascorbic acid, and ibuprofen, hardness values varied from what had been previously found in the literature through other bulk techniques, such as bulk impact-rebound methods. They pointed out that within the existing body of literature, different peak depths/loads, indenter geometries, and measurement methodologies are often chosen, confounding direct comparison between studies. Moreover, an indentation size effect on H, where the measured H changes as a function of contact depth, was not observed for ascorbic acid, but was present for the other four crystals. Other work has shown that nanoindentation of sucrose gives hardness values that exceed those measured by nanoindentation by a factor of two [118]. Such size effects have been commonly observed in metallic materials for decades [119], and have been attributed to non-uniform deformation, whereupon a lack of suitable dislocation sources at low indentation depths leads to increased hardness. With increasing depth, the volume of indented material increases until hardness approaches values that would be associated with a bulk large-scale sample.

821

822

823

824

825

826

827

828

829

830

831

832

833

834

835

836

837

838

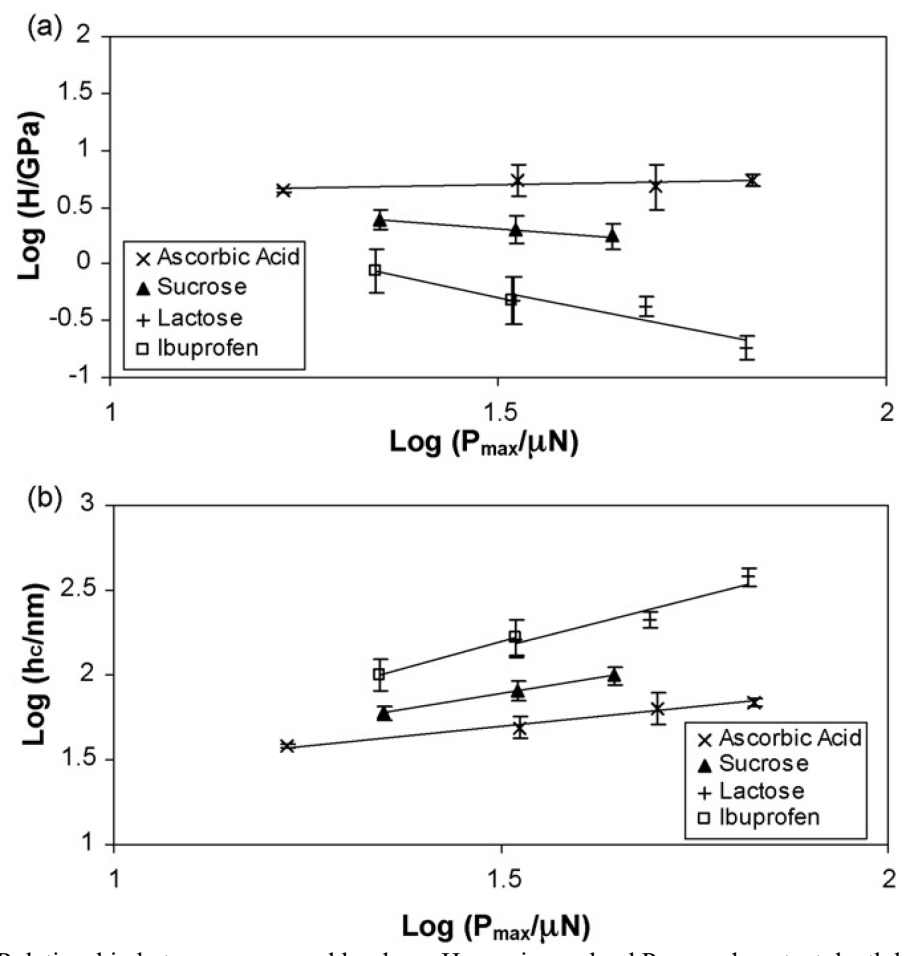


Fig. 21. Relationship between measured hardness H, maximum load P_{max} , and contact depth h_c for four pharmaceutical materials. Note that presentation of data in this manner provides for effective comparison between materials with respect to hardness (a) and contact depth (b) over a range of P_{max} [120].

One method for addressing the inconsistencies in nanohardness values in the literature is by reporting results as shown in Fig. 21. Here, rather than reporting a single value for H over a range of maximum depth or load, hardness may be reported as function of P_{max} . Such an approach has been used in the literature to provide a relative ranking of H [120, 121]. Importantly, it provides for a more direct comparison between materials that may show properties that similarly scale with P_{max} , although at different maximum loads, e.g., lactose and ibuprofen in Fig. 21(a). One may infer that lactose and ibuprofen behave similarly, even though the provided datasets at first glance show that lactose has a lower hardness than ibuprofen until the load range and size effect is accounted for.

4.2.6 Correlative characterization methods

It is well-known that some pharmaceutical crystals can undergo transformation to other polymorphs under applied stress. Manimunda and coworkers [122] investigated stress-induced

phase transformations in aspirin utilizing a nanoindenter integrated with a Raman microscope. Their findings are summarized in Fig. 22, where two Raman peaks and their intensity ratio (Fig. 22(a,b,c)) revealed that transformation from form II into form I occurred at the center of the indentation zone while form I was stable under indentation.



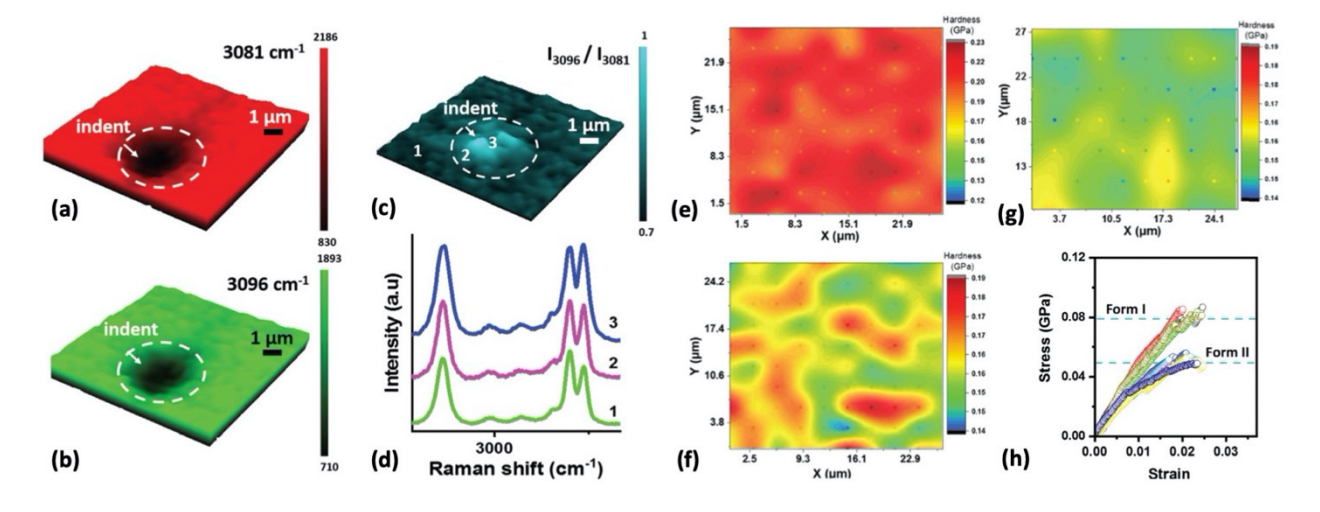


Fig. 22. Raman intensity maps arising from indentation on an aspirin form II {10\overline{2}} surface where (a) is the amplitude variation of the 3081 cm⁻¹ peak, (b) is the amplitude variation of the 3096 cm⁻¹ peak, and (c) is their ratio. The changes in intensity reflect a stress-induced phase transformation from form II to form I at indentation loads higher than 4 mN. (d) shows the three spectra correlated to the positions noted in (c). (e) is a high-throughput hardness map of a form I crystal, (f) is a form II crystal interspersed with form I crystals, and (h) are spherical indentation stress-strain curves for the harder form I and softer form II phases [122].

Using this information, they were able to determine the critical load to drive the form II to form I transformation, and generate hardness maps at sufficiently low load so as to not trigger the phase transformation. This in turn enabled the acquisition of high-throughput hardness maps, whereupon either homogeneous form I $\{100\}$ (Fig. 22(e)), homogeneous Form (II $\{10\overline{2}\}$ (Fig. 22(g)), or a form II microstructure containing embedded form I domains could be imaged according to the mechanical contrast provided by hardness differences between the two phases (Fig. 22(f)). The green and light-yellow fields represent the softer form II, and the red regions belong to form I. The authors combined yet another technique with their comprehensive data set, utilizing spherical nanoindentation stress-strain analysis (Fig. 22(h)) to elucidate differences in both yield point and in work hardening behavior. These two quantities are generally off-limits to the standard Oliver and Pharr approach of determining H and E. This combination of Raman microscopy, mechanical mapping, and spherical nanoindentation provides a superb example of the richness of pharmaceutical material data sets that may be acquired via complementary

nanoindentation techniques. In the aforementioned work, Raman microscopy was applied ex-situ to the indentation event. Raman microscopy techniques have also been extended to in-situ straining geometries, such as during compaction of chlorpropamide [123] microscale beam bending of celecoxib [124], and during nanoindentation at the corner of piroxicam crystals [125].

887

883

884

885

886

5. Conclusion and outlook

888 889 890

891

892

893

894

895

896

897

898

899

900

901

902

903

904

905

906

907

908

909

910

911

912

913

914

Given the criticality of mechanical properties in pharmaceutical formulation design and manufacturing, nanomechanical testing plays an increasingly important role in drug development. The high spatial resolution of nanomechanical testing opens the possibility to obtain fundamental mechanical properties using small specimens, with minimal sample preparation for techniques involving nanoindentation. Modern nanomechanical testing instruments are increasingly capable of probing the response of materials to important external stimuli, such as temperature, humidity, and strain rate which will prove invaluable to development of models that incorporate these conditions into processing protocols. While fundamental theories underlying nanomechanical testing for other classes of materials have been well developed, its reliable applications to pharmaceutical materials requires overcoming unique challenges in sample preparation and anisotropy of molecular crystals. Specifically, to ensure accuracy of measured mechanical properties, common sources of error during nanomechanical testing must be recognized and appropriate measures must be taken to eliminate them when analyzing any pharmaceutical materials. The future of nanomechanical testing of pharmaceutical materials is promising. Several emerging test methods and data analysis protocols, especially in the realm of correlative sitespecific studies and in determination of fundamental rate dependent parameters, such as activation energy and volume for unit deformation processes [79, 108], will prove indispensable in deepening our understanding of structure - property relationships in pharmaceutical materials. Research efforts in this area are expected to grow rapidly and to fill a gap in the journey towards achieving the goal of digital design of drug products. In this approach, a high quality drug product is designed efficiently based on predictive models incorporating physicochemical and mechanical properties of the drug derived from its molecular structure as inputs. Minimal experiments are performed to verify or fine-tune the properties of the drug product. We anticipate that nanomechanical testing will play a crucial role in the development of the predictive models underpinning this approach, as well as quality control of the finished tablet.

916

Declaration of Competing Interest

917 None

References

[1] L.J. Taylor, D.G. Papadopoulos, P.J. Dunn, A.C. Bentham, N.J. Dawson, J.C. Mitchell, M.J. Snowden

Predictive milling of pharmaceutical materials using nanoindentation of single crystals

Org. Proc. Res. Dev., 8 (2004), pp. 674-679, https://doi.org/10.1021/op0300241

[2] M. Meier, E. John, D. Wieckhusen, W. Wirth, W. Peukert

Influence of mechanical properties on impact fracture: Prediction of the milling behaviour of pharmaceutical powders by nanoindentation.

Powder Technol., 188 (2009), pp. 301-313, https://doi.org/10.1016/j.powtec.2008.05.009

[3] C.C. Sun

Decoding Powder Tabletability: Roles of Particle Adhesion and Plasticity J. Adhes. Sci.Technol., 25 (2011), pp. 483-499, https://doi.org/10.1163/016942410X525678

[4] S. Paul, K. Wang, L.J. Taylor, B. Murphy, J. Krzyzaniak, N. Dawson, M.P. Mullarney, P. Meenan, C.C. Sun

Dependence of Punch Sticking on Compaction Pressure-Roles of Particle Deformability and Tablet Tensile Strength

J. Pharm. Sci., 106 (2017), pp. 2060-2067, https://doi.org/10.1016/j.xphs.2017.04.059

[5] C.K. Tye, C.C. Sun, G.E. Amidon

Evaluation of the effects of tableting speed on the relationships between compaction pressure, tablet tensile strength, and tablet solid fraction

J. Pharm. Sci., 94 (2005), pp. 465-472, https://doi.org/10.1002/jps.20262

[6] S. Paul, C. G. Wang, C.C. Sun

Tabletability Flip - Role of Bonding Area and Bonding Strength Interplay J. Pharm. Sci., 109 (2020), pp. 3569-3573, https://doi.org/10.1016/j.xphs.2017.04.059

[7] C.C. Sun

A classification system for tableting behaviors of binary powder mixtures Asian J. Pharm. Sci., 11 (2016), pp. 486-491, https://doi.org/10.1002/jps.21552

[8] C.C. Sun

Materials Science Tetrahedron-A Useful Tool for Pharmaceutical Research and Development

J. Pharm. Sci., 98 (2009), pp. 1671-1687, https://doi.org/10.1002/jps.21552

[9] S. Saha, M.K. Mishra, C.M. Reddy, G.R. Desiraju

From Molecules to Interactions to Crystal Engineering: Mechanical Properties of Organic Solids

Acc. Chem. Res., 51 (2018), pp. 2957-2967, https://doi.org/10.1021/acs.accounts.8b00425

[10] A.C. Fischer-Cripps

Applications of Nanoindentation	In: Nanoindentation.	Mechanical Engir	neering Series
Springer, New York, NY., 2011, ht	tps://doi.org/10.1007	⁷ /s11837-018-2752	2-0

- [11] E.D. Hintsala, U. Hangen, D.D. Stauffer
 High-Throughput Nanoindentation for Statistical and Spatial Property
 Determination
- JOM, 70 (2018), pp. 494-503, https://doi.org/10.1007/s11837-018-2752-0
 [12] J.M. Katz, I.S. Buckner
 - Characterization of strain rate sensitivity in pharmaceutical materials using indentation creep analysis
 - Int. J. Pharm., 2013. 442 (2013), pp. 13-19, https://doi.org/10.1007/s11837-018-2752-0
- [13] J. Alkorta, J.M. Martinez-Esnaola, J.G. Sevillano
 Critical examination of strain-rate sensitivity measurement by nanoindentation methods: Application to severely deformed niobium.
 Acta Mater., 56 (2008), pp. 884-893, https://doi.org/10.1016/j.actamat.2007.10.039
- [14] V. Maier, K. Durst, J. Mueller, B. Backes, H.W. Höppel, M. Göken

 Nanoindentation strain-rate jump tests for determining the local strain-rate
 sensitivity in nanocrystalline Ni and ultrafine-grained Al

 J. Mater. Res., 26 (2011), pp. 1421-1430, 10.1557/jmr.2011.156
- [15] V. Maier, B. Merle, M. Göken, K. Durst
 An improved long-term nanoindentation creep testing approach for studying the local deformation processes in nanocrystalline metals at room and elevated temperatures
 J. Mater. Res., 28 (2013), pp. 1177-1188, 10.1557/jmr.2013.39
- [16] B.N. Lucas, W.C. Oliver

 Indentation power-law creep of high-purity indium

 Metall. Mater. Trans. A Phys. Metall. Mater. Sci., 30 (1999), pp. 601-610, https://doi.org/10.1007/s11661-999-0051-7
- [17] H.G. Jung, D. Lee, S.W. Lee, I. Kim, Y. Kim, J.W. Jang, J.H. Lee, G. Lee, D.S. Yoon Nanoindentation for Monitoring the Time-Variant Mechanical Strength of Drug-Loaded Collagen Hydrogel Regulated by Hydroxyapatite Nanoparticles

 ACS Omega, 6 (2021), pp. 9269-9278, https://doi.org/10.1021/acsomega.1c00824
- [18] M.S. Lamm, A. Simpson, M. McNevin, C. Frankenfield, R. Nay, N. Variankaval Probing the Effect of Drug Loading and Humidity on the Mechanical Properties of Solid Dispersions with Nanoindentation: Antiplasticization of a Polymer by a Drug Molecule
- Mol. Pharm., 9 (2012), pp. 3396-3402, https://doi.org/10.1021/mp3003013
 [19] M.L.B Palacio, B. Bhushan, B
- [19] M.L.B Palacio, B. Bhushan, B

 Depth-sensing indentation of nanomaterials and nanostructures

 Mater. Charact., 78 (2013), pp. 1-20, https://doi.org/10.1515/acph-2016-0032
- [20] S. Patel, X. Kou, H.H. Hou, Y.B. Huang, J.C. Strong, G.G.Z. Zhang, C.C. Sun Mechanical Properties and Tableting Behavior of Amorphous Solid Dispersions J. Pharm. Sci., 106 (2017), pp. 217-223, 10.1016/j.xphs.2016.08.021
- [21] M. Egart, B. Jankovic, S. Srcic

 Application of instrumented nanoindentation in preformulation studies of pharmaceutical active ingredients and excipients

 Acta Pharm., 66 (2016), pp. 303-330, 10.1039/C3CE41266K

[22] S. Varughese, M.S.R.N. Kiran, U. Ramamurty, G.R. Desiraju
Nanoindentation in Crystal Engineering: Quantifying Mechanical Properties of Molecular Crystals
Angew. Chem. Int. Ed., 52 (2013), pp. 2701-2712, https://doi.org/10.1088/0508-3443/7/5/301

[23] U. Ramamurty, and J.I. Jang
Nanoindentation for probing the mechanical behavior of molecular crystals-a review of the technique and how to use it
CrystEngComm, 16 (2014), pp. 12-23, 10.1039/C3CE41266K

[24] D. Tabor

The Physical Meaning of Indentation and Scratch Hardness Br. J. Appl. Phys., 7 (1956), pp. 159-166.

[25] D. Tabor

The hardness of metals (Oxford University Press, 1951), 2000. https://doi.org/10.1088/0508-3443/7/5/301

[26] M.R. VanLandingham

Review of instrumented indentation

J. Res. Natl. Inst. Stand. Technol., 108 (2003), p. 249-265, https://dx.doi.org/10.6028%2Fjres.108.024

[27] W.C. Oliver, and G.M. Pharr

An Improved Technique for Determining Hardness and Elastic-Modulus Using Load and Displacement Sensing Indentation Experiments
J. Mater. Res., 7 (1992), pp. 1564-1583, 10.1557/JMR.1992.1564

[28] N.R. Moody, W.W. Gerberich, N. Burnham, S.P. Baker **Fundamentals of nanoindentation and nanotribology** Mater. Res. Soc., 1998, Warrendale, PA.

[29] W.C. Oliver, G.M. Pharr

Measurement of hardness and elastic modulus by instrumented indentation: Advances in understanding and refinements to methodology

J. Mater. Res., 19 (2004), pp. 3-20, 10.1557/jmr.2004.19.1.3

[30] J.C. Hay, A. Bolshakov, G.M. Pharr

A critical examination of the fundamental relations used in the analysis of nanoindentation data

J. Mater. Res., 14 (1999), pp. 2296-2305, 10.1557/JMR.1999.0306

[31] Y.T. Cheng, C.M Cheng

Scaling approach to conical indentation in elastic-plastic solids with work hardening J. Appl. Phys., 84 (1998), pp. 1284-1291, https://doi.org/10.1063/1.368196

[32] L. Riester, R.J. Bridge, K. Breder
Characterization of vickers, berkovich, spherical and cube cornered diamond indenters by nanoindentation and sfm
MRS Online Proceedings Library, (1998), https://doi.org/10.1557/PROC-522-45

[33] T. Chudoba, P. Schwaller, R. Rabe, J.M. Breguet, J. Michler

Comparison of nanoindentation results obtained with Berkovich and cube-corner
Indenters
Philos. Mag., 86 (2006), pp. 33-35, https://doi.org/10.1080/14786430600746424

[34] C.A. Tweedie, K.J. Van Vliet

Contact creep compliance of viscoelast	tic materials via nanoindentation
J. Mater. Res., 21 (2006), pp. 1576-1589	, https://doi.org/10.1557/jmr.2006.0197

- [35] M.L. Oyen, R.F. Cook Load-displacement behavior during sharp indentation of viscous-elastic-plastic Materials J. Mater. Res., 18 (2003), pp. 139-50, https://doi.org/10.1557/JMR.2003.0020
- [36] E.G. Herbert, W.C. Oliver, A. Lumsdaine, G.M. Pharr Measuring the constitutive behavior of viscoelastic solids in the time and frequency domain using flat punch nanoindentation J. Mater. Res., 24 (2011), pp. 626-637, https://doi.org/10.1557/jmr.2009.0089
- [37] G.F. Wang, X.R. Niu

 Nanoindentation of soft solids by a flat punch
 Acta Mech. Sin., 31 (2015), pp. 531-535, https://doi.org/10.1007/s10409-015-0440-7
- [38] X.D. Li, B. Bhushan
 A review of nanoindentation continuous stiffness measurement technique and its applications
 Mater. Charact., 48 (2002), pp. 11-36, https://doi.org/10.1016/S1044-5803(02)00192-4
- [39] S.J. Vachhani, R.D. Doherty, S.R. Kalidindi

 Effect of the continuous stiffness measurement on the mechanical properties

 extracted using spherical nanoindentation

 Acta Mater., 61 (2013), pp. 3744-3751, https://doi.org/10.1016/j.actamat.2013.03.005
- [40] K. Durstand, V. Maier

 Dynamic nanoindentation testing for studying thermally activated processes from single to nanocrystalline metals

 Curr. Opin. Solid State Mater. Sci., 19 (2015), pp. 340-353, https://doi.org/10.1016/j.cossms.2015.02.001
- [41] G.M. Odegard, T.S. Gates, H.M. Herring
 Characterization of viscoelastic properties of polymeric materials through
 Nanoindentation
 Exp. Mech., 45 (2005), pp. 130-136, https://doi.org/10.1007/BF02428185
- [42] K. Hu, P. Radhakrishnan, R.V. Patel, J.J. Mao
 Regional structural and viscoelastic properties of fibrocartilage upon dynamic
 nanoindentation of the articular condyle
 J. Struct. Biol., 136 (2001), pp. 46-52, https://doi.org/10.1006/jsbi.2001.4417
- [43] S.A. Hayes, A.A. Goruppa, F.R. Jones

 Dynamic nanoindentation as a tool for the examination of polymeric materials

 J. Mater. Res., 19 (2004), pp. 3298-3306, 10.1557/JMR.2004.0437
- [44] M.R. VanLandingham, J.S. Villarrubia, W.F. Guthrie, G.F. Meyers Nanoindentation of polymers: an overview Macromol. Symp., 167 (2001), pp. 15-44, https://doi.org/10.1002/1521-3900(200103)167:1%3C15::AID-MASY15%3E3.0.CO;2-T
- [45] J. Sun, W. Wu, M. Ling, B. Bhushan, J. Tong
 A dynamic nanoindentation technique to investigate the nanomechanical properties
 of a colored beetle
 RSC Adv., 6 (2016), pp. 79106-79113, https://doi.org/10.1039/C6RA14687B
- [46] C.G. Wang, C.C. Sun

The landscape of mecha	unical properties of	f molecular crystals	
CrystEngComm, 22 (202	0), pp. 1149-1153, 1	https://doi.org/10.1039/C9CE0)1874C

- [47] M.K. Mishra, U. Ramamurty, G.R. Desiraju

 Hardness Alternation in alpha,omega-Alkanedicarboxylic Acids

 Chem. Asian J., 10 (2015), pp. 2176-81, https://doi.org/10.1002/asia.201500322
- [48] M.K. Mishra, S. Varughese, U. Ramamurty, G.R. Desiraju

 Odd-even effect in the elastic modulii of alpha,omega-alkanedicarboxylic acids

 J. Am. Chem. Soc., 135 (2013), pp. 8121-8124, https://doi.org/10.1021/ja402290h
- [49] M.K. Mishra, U. Ramamurty, G.R. Desiraju

 Mechanical property design of molecular solids

 Curr. Opin. Solid State Mater. Sci., 20 (2016), pp. 361-370, https://doi.org/10.1016/j.cossms.2016.05.011
- [50] P. Sanphui, M.K. Mishra, U. Ramamurty, G.R. Desiraju **Tuning Mechanical Properties of Pharmaceutical Crystals with Multicomponent Crystals: Voriconazole as a Case Study**Mol. Pharm., 12 (2015), pp. 889-897, https://doi.org/10.1021/mp500719t
- [51] C.G. Wang, S.Y. Hu, C.C. Sun
 Expedited development of a high dose orally disintegrating metformin tablet
 enabled by sweet salt formation with accsulfame
 Int. J. Pharm., 532 (2017), pp. 435-443, https://doi.org/10.1016/j.ijpharm.2017.08.100
- [52] J.P. Yadav, R.N. Yadav, P. Uniyal, H. Chen, C. Wang, C.C. Sun Molecular Interpretation of Mechanical Behavior in Four Basic Crystal Packing of Isoniazid with Homologous Cocrystal Formers Cryst. Growth Des., 20 (2020), pp. 832-844, https://doi.org/10.1021/acs.cgd.9b01224
- [53] B.P. Gabriella, C.J. Williams, M.E. Lauer, B. Derby, A.J. Cruz-Cabeza
 Impact of polymorphism on mechanical properties of molecular crystals: a study of
 p-amino and p-nitro benzoic acid with nanoindentation
 CrystEngComm, 23 (2021), pp. 2027-2033, https://doi.org/10.1039/D1CE00041A
- [54] M.K. Mishra, P. Sanphui, U. Ramamurty, G.R. Desiraju Solubility-Hardness Correlation in Molecular Crystals: Curcumin and Sulfathiazole Polymorphs Cryst. Growth Des., 14 (2014), pp. 3054-3061, https://doi.org/10.1021/cg500305n
- [55] C.C. Sun, D.J.W. Grant
 Influence of crystal structure on the tableting properties of sulfamerazine polymorphs
 - Pharm. Res., 18 (2001), pp. 274-280, https://doi.org/10.1023/A:1011038526805
- [56] K.M. Picker-Freyer, X. Liao, G. Zhang, T.S. Wiedmann **Evaluation of the compaction of sulfathiazole polymorphs**Journal of Pharmaceutical Sciences, 96 (2007), pp. 2111-2124, https://doi.org/10.1002/jps.21042
- [57] C. Wang, S. Paul, K. Wang, S. Hu, C.C. Sun
 Relationships among Crystal Structures, Mechanical Properties, and Tableting
 Performance Probed Using Four Salts of Diphenhydramine
 Cryst. Growth Des., 17 (2017), pp. 6030-6040, https://doi.org/10.1021/acs.cgd.7b01153
- [58] C. Wang, S. Paul, D.J. Sun, S.O. Nilsson Lill, C.C. Sun

Mitigating Punch Sticking Propensity of Celecoxib by Cocrystallization: An	n
Integrated Computational and Experimental Approach	

Cryst. Growth Des., 20 (2020), pp. 4217-4223, https://doi.org/10.1021/acs.cgd.0c00492

- [59] B.R. Rohrs, G.E. Amidon, R.H. Meury, P.J. Secreast, H.M. King, C.J. Skoug Particle size limits to meet USP content uniformity criteria for tablets and capsules J. Pharm. Sci., 95 (2006), pp. 1049-1059, https://doi.org/10.1002/jps.20587
- [60] C. Jacobs, R.H. Muller

Production and characterization of a budesonide nanosuspension for pulmonary administration

Pharm. Res., 19 (2002), pp. 189-194, https://doi.org/10.1021/acs.cgd.7b01153

[61] A.A. Noyes, W.R. Whitney

The rate of solution of solid substances in their own solutions

J. Am. Chem. Soc., 19 (1897), pp. 930-934, http://dx.doi.org/10.1021/ja02086a003

[62] E. Merisko-Liversidge, G.G. Liversidge

Nanosizing for oral and parenteral drug delivery: A perspective on formulating poorly-water soluble compounds using wet media milling technology Adv. Drug Deliv. Rev., 63 (2011), pp. 427-440, https://doi.org/10.1016/j.addr.2010.12.007

- [63] C.C. Kwan, Y.Q. Chen, Y.L. Ding, D.G. Papadopoulos, A.C. Bentham, M. Ghadiri Development of a novel approach towards predicting the milling behaviour of pharmaceutical powders
 - Eur. J. Pharm. Sci., 23 (2004), pp. 327-336, https://doi.org/10.1016/j.ejps.2004.08.006
- [64] M.R. Taw, J.D. Yeager, D.E. Hooks, T.M. Carvajal, D.F. Bahr The mechanical properties of as-grown noncubic organic molecular crystals assessed by nanoindentation

J. Mater. Res., 32 (2017), pp. 2728-2737, 10.1557/jmr.2017.219

- [65] B.P. Gabriele, C.J. Williams, D. Stauffer, B. Derby, A.J. Cruz-Cabeza

 Brittle Behavior in Aspirin Crystals: Evidence of Spalling Fracture

 Cryst. Growth Des., 21 (2021), pp. 1786-1790, https://doi.org/10.1021/acs.cgd.0c01662
- [66] C.B. Ponton, R.D. Rawlings
 Vickers Indentation Fracture-Toughness Test .1. Review of Literature and

Formulation of Standardized Indentation Toughness Equations
Mater. Sci. Technol, 5 (1989), pp. 865-872, https://doi.org/10.1179/mst.1989.5.9.865

[67] C.B. Ponton, R.D. Rawlings

Vickers Indentation Fracture-Toughness Test .2. Application and Critical-Evaluation of Standardized Indentation Toughness Equations

Mater. Sci. Technol, 5 (1989), pp. 961-976, https://doi.org/10.1179/mst.1989.5.10.961

[68] S. Varughese, M.S.R.N. Kiran, K.A. Solanko, A.D. Bond, U. Ramamurty, G.R. Desiraju Interaction anisotropy and shear instability of aspirin polymorphs established by nanoindentation

Chem. Sci., 2 (2011), pp. 2236-2242, https://doi.org/10.1039/C1SC00430A

- [69] M. Kiran, S. Varughese, C.M. Reddy, U. Ramamurty, G.R. Desiraju Mechanical Anisotropy in Crystalline Saccharin: Nanoindentation Studies Cryst. Growth Des., 10 (2010), pp. 4650-4655, https://doi.org/10.1021/cg1009362
- [70] M.K. Mishra, G.R. Desiraju, U. Ramamurty, A.D. Bond

Studying Microstructure in Molecular Crystals With Nanoindentation: Intergrowth Polymorphism in Felodipine

Angew. Chem. Int. Ed., 53 (2014), pp. 13102-13105, https://doi.org/10.1002/ange.201406898

[71] R.M. Mohamed, M.K. Mishra, L.M. Al-Harbi, M.S. Al-Ghamdi, U. Ramamurty Anisotropy in the mechanical properties of organic crystals: temperature dependence

Rsc Adv., 2015. 5 (2015), pp. 64156-64162, https://doi.org/10.1039/C5RA11656B

[72] A. Newman,

Pharmaceutical amorphous solid dispersions John Wiley & Sons, 2015.

- [73] N. Shah, H. Sandhu, D.S. Choi, H. Chokshi, A.W. Malick

 Amorphous Solid Dispersions In: Advances in Delivery Science and Technology,
 Springer, New York, NY.
- [74] A.M. Diez-Pascual, M.A. Gómez-Fatou, F. Ania, A. Flores
 Nanoindentation in polymer nanocomposites
 Prog. Mater. Sci., 67 (2015), pp. 1-94, https://doi.org/10.1016/j.pmatsci.2014.06.002
- [75] M.D.L.L.R Medina, V. Kumar Evaluation of cellulose II powders as a potential multifunctional excipient in tablet formulations

Int. J. Pharm., 322 (2006), pp. 31-35, https://doi.org/10.1016/j.ijpharm.2006.05.033

- [76] S.J. Strydom, D.P. Otto, W. Liebennerg, Y.M. Lvov, M.M. De Villiers

 Preparation and characterization of directly compactible layer-by-layer nanocoated cellulose
 - Int. J. Pharm., 404 (2011), pp. 57-65, https://doi.org/10.1016/j.ijpharm.2010.10.056

[77] B. Govedarica, I. Ilić, S. Srčič

The use of single particle mechanical properties for predicting the compressibility of pharmaceutical materials

Powder Technol., 225 (2012), pp. 43-51, https://doi.org/10.1016/j.powtec.2012.03.030

[78] W.J. Sun, S. Kothari, C.C. Sun

The relationship among tensile strength, Young's modulus, and indentation hardness of pharmaceutical compacts

Powder Technol., 331 (2018), pp. 1-6, https://doi.org/10.1016/j.powtec.2018.02.051

- [79] K.M. Schmalbach, A.C. Lin, D.C. Bufford, C. Wang, C.C. Sun, N.A. Mara Nanomechanical mapping and strain rate sensitivity of microcrystalline cellulose J. Mater. Res., **36** (2021), pp. 2251-2265, https://doi.org/10.1557/s43578-021-00138-0
- [80] F. Bassam, P. York, R.C. Rowe, R.J. Roberts Young's modulus of powders used as pharmaceutical excipients Int. J. Pharm., 64 (1990), pp. 55-60, https://doi.org/10.1016/0378-5173(90)90178-7

[81] K.L. Johnson

Contact Mechanics

Cambridge University Press, 1987.

[82] A.R. Emeje Martins Ochubiojo

Starch: From food to medicine Benjamin Valdez, In: Scientific, health and social aspects of the food industry, 2011.

- [83] H. Mohammed, B.J. Briscoe, K.G. Pitt

 The intrinsic nature and the coherence of compacted pure pharmaceutical tablets
 Powder Technol., 165 (2006), pp. 11-21, https://doi.org/10.1016/j.powtec.2006.03.010
- [84] N. Al-Zoubi, A. Ardakani, F. Odeh, N. Sakhnini, I. Partheniadis, I. Nikolakakis Mechanical properties of starch esters at particle and compact level Comparisons and exploration of the applicability of Hiestand's equation to predict tablet strength. Eur. J. Pharm. Sci., 147 (2020), 105292, https://doi.org/10.1016/j.ejps.2020.105292
- [85] K. Flügel, K. Schmidt, L. Mareczek, M. Gäbe, R. Hennig, M. Thommes Impact of incorporated drugs on material properties of amorphous solid dispersions.

Eur. J. Pharm. Biopharm., 159 (2021), pp. 88-98, https://doi.org/10.1016/j.ejpb.2020.12.017

[86] L.R. Hilden, K.R. Morris, K.R **Physics of amorphous solids**J. Pharm. Sci., 93 (2004), pp. 3-12, https://doi.org/10.1002/jps.10489

[87] K. Flugel, R. Hennig, M. Thommes

Impact of structural relaxation on mechanical properties of amorphous polymers

Eur. J. Pharm. Biopharm., 154 (2020), pp. 214-221,

https://doi.org/10.1016/j.ejpb.2020.07.016

[88] A.N. Zaid

A Comprehensive Review on Pharmaceutical Film Coating: Past, Present, and Future

Drug Des. Devel.Ther., 14 (2020), pp. 4613-4623, https://dx.doi.org/10.2147%2FDDDT.S277439

[89] S.C. Porter, L.A. Felton

Techniques to assess film coatings

Drug Day, Ind. Pharm. 36 (2010) at

Techniques to assess film coatings and evaluate film-coated products. Drug Dev. Ind. Pharm., 36 (2010), pp. 128-142, https://doi.org/10.3109/03639040903433757

[90] G. Perfetti, J. Arfsten, A. Kwade, W.J. Wildeboer, G.M.H. Meesters
Repeated Impacts Tests and Nanoindentation as Complementary Tools for
Mechanical Characterization of Polymer-Coated Particles
J. Appl. Polym. Sci., 118 (2010), pp. 790-804, https://doi.org/10.1002/app.32215

[91] L.M. Shi, C.C. Sun

Overcoming Poor Tabletability of Pharmaceutical Crystals by Surface Modification Pharm. Res., 28 (2011), pp. 3248-3255, https://doi.org/10.1007/s11095-011-0518-2

[92] R.M. Mohamed, M.K. Mishra, L.M. Al-Harabi, M.S. Al-Ghamdi, A.M. Asiri, C.M. Reddy, U. Ramamurty

Temperature Dependence of Mechanical Properties in Molecular Crystals Cryst. Growth Des., 15 (2015), pp. 2474-2479, https://doi.org/10.1021/acs.cgd.5b00245

[93] H. Liu, L. Yu, X.Z. Xiao

Hardness-Depth Relationship with Temperature Effect for Single Crystals-A Theoretical Analysis

Crystals, 10 (2020), https://doi.org/10.3390/cryst10020112

[94] C. Ganser, U. Hirn, S. Rohm, R. Schennach, C. Teichert **AFM nanoindentation of pulp fibers and thin cellulose films at varying relative humidity**

	Holzforschung, 68 (2014), pp. 53-60, https://doi.org/10.1515/hf-2013-0014
[95]	A.C. Fischer-Cripps
	Critical review of analysis and interpretation of nanoindentation test data
	Surf. Coat. Tech., 200 (2006), pp. 4153-4165,
	https://doi.org/10.1016/j.surfcoat.2005.03.018
[96]	S. Pathak, S.R. Kalidindi
	Spherical nanoindentation stress-strain curves
	Mater. Sci. Eng., 91 (2015), pp. 1-36, https://doi.org/10.1016/j.mser.2015.02.001
[97]	J.S. Weaver, C. Sun, Y. Wang, S.R. Kalidindi, R.P. Doerner, N.A. Mara, S. Pathak
	Quantifying the mechanical effects of He, W and He + Wion irradiation on tungsten
	with sphericalnanoindentation
	J. Mater. Sci., 53 (2018), pp. 5296-5316, https://doi.org/10.1007/s10853-017-1833-8
[98]	S. Pathak, S.R. Kalidindi, N.A. Mara
	Investigations of orientation and length scale effects on micromechanical responses
	in polycrystalline zirconium using spherical nanoindentation
	Scr. Mater., 113 (2016), pp. 241-245, https://doi.org/10.1016/j.scriptamat.2015.10.035
[99]	S. Pathak, S.J. Vachhani, K.J. Jepsen, H.M. Goldman, S.R. Kalidindi
	Assessment of lamellar level properties in mouse bone utilizing a novel spherical
	nanoindentation data analysis method
	J. Mech. Behav. Biomed. Mater., 13 (2012), pp. 102-117,
	https://dx.doi.org/10.1016%2Fj.jmbbm.2012.03.018
[100]	L.W. Yang, C.R. Mayer, N. Chawla, J. LLorca, J.M. Molina- Aldareguía
	Nanomechanical characterization of the fracture toughness of Al/SiC nanolaminates
F4.0.4.7	Extreme Mech. Lett., 40 (2020). https://doi.org/10.1016/j.eml.2020.100945
[101]	D.S. Gianola, C. Eberl
	Micro- and nanoscale tensile testing of materials
F1 0 0 1	JOM, 61 (2009), pp. 24-35, https://doi.org/10.1007/s11837-009-0037-3
[102]	N.A. Mara, D. Bhattacharya, P. Dickerson, R.G. Hoagland, A. Misra, A
	Deformability of ultrahigh strength 5nm Cu/Nb nanolayered composites
F1021	Appl. Phys. Lett., 92 (2008), pp. 231901(1-3), https://doi.org/10.1063/1.2938921
[103]	D. Raut, M.S.R.N. Kiran, M.K. Mishra, A.M. Asiri, U. Ramamurty
	On the loading rate sensitivity of plastic deformation in molecular crystals
F1041	Cryst. Eng. Comm., 18 (2016), pp. 3551-3555, https://doi.org/10.1039/C6CE00575F
[104]	S. Varughese, M.S. Kiran, U. Ramamurty, G.R. Desiraju Nanoindentation as a probe for mechanically-induced molecular migration in
	layered organic donor-acceptor complexes
	Chem. Asian J., 7 (2012), pp. 2118-2125, https://doi.org/10.1002/asia.201200224
[105]	V. Maier-Kiener, K. Durst
[103]	Advanced Nanoindentation Testing for Studying Strain-Rate Sensitivity and
	Activation Volume
	JOM, 69 (2017), pp. 2246-2255, https://doi.org/10.1007/s11837-017-2536-y
	1 3 1.1. (3) (-3 1 /) pp. 22 10 22 0 ; <u>interpolit delivery 10 110 0 / 01 / 20 0 / </u>

[106] M.J. Mayo, W.D. Nix

 A micro-indentation study of superplasticity in Pb, Sn, and Sn-38 wt% Pb
 Acta Metall., 36 (1988), pp. 2183-2192, https://doi.org/10.1016/0001-6160(88)90319-7

 [107] G.B. Gibbs

The activation parameters for dislocation glide

Philos. Mag., 16 (1967), pp	. 97-102, https://doi.org	<u>;/10.1080/14786436708229259</u>

[108] M.S.R.N. Kiran, M.K. Mishra, U. Ramamurty

Activation Volume of the Elastic-Plastic Transition in Molecular Crystals

Cryst. Growth Des., 21 (2021), pp. 5183-5191, https://doi.org/10.1021/acs.cgd.1c00543

[109] C.A. Schuh, A.C. Lund

Application of nucleation theory to the rate dependence of incipient plasticity during nanoindentation

J. Mater. Res., 19 (2011), pp. 2152-2158, https://doi.org/10.1557/JMR.2004.0276

[110] J.K. Mason, A.C. Lund, C.A. Schuh

Determining the activation energy and volume for the onset of plasticity during Nanoindentation

Phys. Rev. B, 73 (2006), pp. 054102, 10.1103/PhysRevB.73.054102

[111] B. Lawn, R. Wilshaw

Indentation Fracture - Principles and Applications

J. Mater. Sci., 10 (1975), pp. 1049-1081, https://doi.org/10.1007/BF00823224

[112] S. Mannepalli, K.S. Mangalampalli

Indentation Plasticity and Fracture Studies of Organic Crystals

Crystals, 7 (2017), pp. 324, https://doi.org/10.3390/cryst7110324

[113] B.R. Lawn, D.B. Marshall

Hardness, Toughness, and Brittleness: An Indentation Analysis

J. Am. Ceram. Soc., 62 (1979), pp. 347-350, https://doi.org/10.1111/j.1151-2916.1979.tb19075.x

[114] D.J. Morris, S.B. Myers, R.F. Cook, R.F.

Sharp probes of varying acuity: Instrumented indentation and fracture behavior J. Mater. Res., 19 (2004), pp. 165-175, 10.1557/jmr.2004.19.1.165

[115] A.C. Burch, J.D. Yeager, D.F. Bahr

Indentation fracture behavior of energetic and inert molecular crystals J. Mater. Res., 34 (2019), pp. 3954-3963, 10.1557/jmr.2019.345

[116] J. Jang, G.M. Pharr

Influence of indenter angle on cracking in Si and Ge during nanoindentation Acta Mater., **56** (2008), pp. 4458-4469, https://doi.org/10.1016/j.actamat.2008.05.005

[117] D.J. Morris, R.F. Cook

Radial fracture during indentation by acute probes: I, description by an indentation wedging model

Int. J. Fract., 136 (2005), pp. 237-264, https://doi.org/10.1007/s10704-005-6034-9

[118] K.J. Ramos, D.F. Bahr

Mechanical behavior assessment of sucrose using nanoindentation

J. Mater. Res., 22 (2007), pp. 2037-2045, 10.1557/jmr.2007.0249

[119] W.D. Nix, H.J. Gao, H.J.

Indentation size effects in crystalline materials: A law for strain gradient plasticity J. Mech. Phys. Solids, 46 (1998), pp. 411-425, https://doi.org/10.1016/S0022-5096(97)00086-0

[120] V.M. Masterson, X.P. Cao

Evaluating particle hardness of pharmaceutical solids using AFM nanoindentation Int. J. Pharm., 2008. 362 (2008), pp. 163-171,

https://doi.org/10.1016/j.ijpharm.2008.06.015

[121] X.M. Liao, T.S. Wiedmann

Measurement of process-dependent material properties of pharmaceutical solids by nanoindentation

- J. Pharm. Sci., 94 (2005), pp. 79-92, https://doi.org/10.1002/jps.20227
- [122] P. Manimunda, S.S. Asif, M.K. Mishra

Probing stress induced phase transformation in aspirin polymorphs using Raman spectroscopy enabled nanoindentation

ChemComm., 55 (2019), pp. 9200-9203, https://doi.org/10.1039/C9CC04538D

[123] H. Park, H. Nie, A. Dhiman, V. Tomar, Q.T. Zhou

Understanding Dynamics of Polymorphic Conversion during the Tableting Process Using In Situ Mechanical Raman Spectroscopy

Mol. Pharm., 17 (2020), pp. 3043-3052,

https://doi.org/10.1021/acs.molpharmaceut.0c00460

[124] K.L. Wang, M.K. Mishra, C.C. Sun

Exceptionally Elastic Single-Component Pharmaceutical Crystals

Chem. Mater., 31 (2019), pp. 1794-1799, https://doi.org/10.1021/acs.chemmater.9b00040

[125] P. Manimunda, E. Hintsala, S. Asif, M.K. Mishra

Mechanical Anisotropy and Pressure Induced Structural Changes in Piroxicam Crystals Probed by In Situ Indentation and Raman Spectroscopy

JOM, 69 (2017), pp. 57-63, https://doi.org/10.1007/s11837-016-2169-6